



CHALMERS
UNIVERSITY OF TECHNOLOGY



Improvement of decal transfer method for preparing fast and reliable CCM assembly

Master's thesis in Materials chemistry

ADAM HURTIG

DEPARTMENT OF PHYSICS

CHALMERS UNIVERSITY OF TECHNOLOGY
Gothenburg, Sweden 2024
www.chalmers.se

MASTER'S THESIS 2024

Improvement of decal transfer method for preparing fast and reliable CCM assembly

ADAM HURTIG



CHALMERS
UNIVERSITY OF TECHNOLOGY

Department of Physics
CHALMERS UNIVERSITY OF TECHNOLOGY
Gothenburg, Sweden 2024

Improvement of decal transfer method for preparing fast and reliable CCM assembly
ADAM HURTIG

© ADAM HURTIG, 2024.

Supervisor: Parinaz Mikaeili, PowerCell Group
Examiner: Björn Wickman, Department of Physics

Master's Thesis 2024
Department of Physics
Chalmers University of Technology
SE-412 96 Gothenburg
Telephone +46 31 772 1000

Typeset in L^AT_EX
Printed by Chalmers Reproservice
Gothenburg, Sweden 2024

Improvement of decal transfer method for preparing fast and reliable CCM assembly
ADAM HURTIG
Department of Physics
Chalmers University of Technology

Abstract

As sustainable energy solutions have garnered more importance in society and to governmental bodies, a technology getting attention as being part of the solution and a step in the right direction is the proton exchange membrane fuel cell (PEMFC). This comes as the PEMFC uses hydrogen and oxygen to create electricity, with the side-products being heat and water, which means that it is a very clean energy converter. At the heart of the fuel cell is the catalyst coated membrane (CCM), which is where the reactions take place, and it is the component investigated in this thesis. Although there are multiple ways of fabricating CCMs, the method used in this thesis is the decal transfer method. Using this method, parameters such as temperature and pressure were varied to investigate the optimal parameters under different conditions. These conditions included the usage of different membranes, three different cathode loadings and two CCM areas. During this process, several analytical tools were employed, with the intent of finding the most effective quality check method for in-house production of CCMs. This included the usage of an optical microscope, lightboard and high intensity light. The performance of CCMs assembled using optimized parameters was also examined by in-situ fuel cell testing. Lastly, an investigation into the most appropriate pressure pad material was performed. The results in this thesis outlines the optimal parameters for each condition and proposes both the most effective quality check method and the most suitable pressure pad material.

Keywords: proton exchange membrane fuel cell, catalyst coated membrane, decal transfer.

Acknowledgements

I would first and foremost like to thank my supervisor Parinaz Mikaeili for her close support and guidance throughout this entire work. Thanks for showing me the ropes and helping me in anything from designing the experiments to evaluating the results, it has been tremendously appreciated. Additionally, I would like to thank Joel Sternberg, Sandeep Jayaprakash Nair and Gabor Toth at Powercell. Joel for your help in introducing some of the analytical tools used in this thesis and for helping me perform measurements such as in-situ. To Sandeep for his efforts in trying to supply my endless demand of electrodes and to Gabor for his help in interpreting results. Lastly a big thanks to my examiner Björn Wickman for the support and feed-back given over the course of my work.

Adam Hurtig, Gothenburg, June 2024

List of Acronyms

Below is the list of acronyms that have been used throughout this thesis listed in alphabetical order:

ACL	Anode Catalyst Layer
CCL	Cathode Catalyst Layer
CCM	Catalyst Coated Membrane
CL	Catalyst Layer
GDL	Gas Diffusion Layer
HC	Hydrocarbon
HOR	Hydrogen Oxidation Reaction
IR	Infrared
MEA	Membrane Electrode Assembly
NDT	Non-destructive Technique
OCV	Open Circuit Voltage
ORR	Oxygen Reduction Reaction
PEMFC	Proton Exchange Membrane Fuel Cell
SEM	Scanning Electron Microscopy
SOFC	Solid Oxide Fuel Cell
T _g	Glass Transition Temperature
TPB	Triple-phase boundary

Nomenclature

Below is the nomenclature of indices, sets, parameters, and variables that have been used throughout this thesis.

cm^2	Area in square centimeter
mgPt/cm^2	Milligram of platinum per square centimeter
N/cm^2	Pressure in Newton per square centimeter
$^{\circ}\text{C}$	Temperature in degree Celsius
A/cm^2	Ampere per square centimeter



Contents

List of Acronyms	ix
Nomenclature	xi
List of Figures	xv
List of Tables	xvii
1 Introduction	1
1.1 Background	1
1.2 Objective	1
1.3 Importance to Powercell	2
2 Theory	3
2.1 Proton Exchange Membrane Fuel Cell	3
2.2 Membrane Electrode Assembly	4
2.3 Materials of MEA	4
2.3.1 Proton exchange membrane	5
2.3.2 Catalyst layer	5
2.3.3 Gas diffusion layer	5
2.3.4 Decal substrates	6
2.3.5 Pressure distribution pads	6
2.4 CCM Quality Parameters	6
2.4.1 Porosity and pore-size distribution	7
2.4.2 Thickness	7
2.4.3 Homogeneity	7
2.4.4 Cracks	8
2.4.5 Delamination	8
2.4.6 Missing catalyst layer and pinholes	8
2.5 Analytical Techniques	9
2.5.1 Optical microscope	9
2.5.2 Light board	9
2.5.3 High intensity light	9
2.5.4 In-situ testing	9
3 Methods	13
3.1 Decal Transfer Method	13

3.2	Comparison of Analytical Techniques	14
3.3	Commercial CCM Quality	14
3.4	Experimental Matrix for Optimization of Transfer Parameters	14
3.5	Evaluation of Pressure Material	15
3.6	In-situ Testing	16
4	Results	17
4.1	Comparison of Analytical Techniques	17
4.1.1	Light board	17
4.1.2	High intensity light	18
4.1.3	Optical microscope	22
4.2	Commercial Quality Check Using High Intensity Light	24
4.3	Optimization of Transfer Parameters for PFSA Membrane	26
4.3.1	Low loading and small area	26
4.3.2	Middle loading and small area	27
4.3.3	High loading and small area	29
4.3.4	Low loading and large area	29
4.3.5	Middle loading and large area	30
4.3.6	High loading and large area	30
4.3.7	Comparison between loadings	31
4.4	Optimization of Transfer Parameters for HC Membrane	31
4.5	Investigation of Color Defect	33
4.6	Evaluation of Pressure Material	35
4.6.1	Initial tests	35
4.6.2	Tests using optimised parameters	37
4.6.2.1	Cellulose/polyester	37
4.6.2.2	Polyester	38
4.6.2.3	Silicone	38
4.6.2.4	Non-reinforced PTFE	39
4.6.2.5	Non-residual paper	39
4.7	In-situ Measurements	40
5	Conclusion	43
6	Outlook for Further Work	45
A	Appendix 1	I

List of Figures

2.1	Illustration of the flows and reactions occurring in the PEMFC.	4
2.2	Illustration of the different regions in a polarization curve.	10
3.1	Initial matrices for optimization of transfer parameters using varying cathode loading, area, and PFSA membrane.	15
4.1	Analysis of CCM 1, 2 and 3 using the light board.	17
4.2	Analysis of anode for usage in CCM assembly, using the light board.	18
4.3	Analysis of CCM 5 using the light board.	18
4.4	Images comparing CCM 1 using high intensity light and light board respectively.	19
4.5	Images comparing CCM 14 in dark (left) and light (right).	19
4.6	Illustration of areas used from the cathode (left) and anode (right) during the assembly and their corresponding CCM.	20
4.7	High intensity light images during the stages of one-sided assembly: bare anode (top left), anode transferred to membrane (top right), full CCM (bottom left) and focus on defect (bottom right). The green and red rings mark two areas of missing catalyst layer on the anode.	21
4.8	High intensity light image of CCM with artificially added pinhole, seen from cathode (left) and anode side (right).	22
4.9	Illustration showing how the light passes through the CCM in the case of: pinhole, missing CL in close proximity, partly aligned missing CL, aligned missing CL, missing CCL and thinner ACL, and lastly non-defected CCM.	22
4.10	Optical images detailing the width of a crack, area of a missing CL, and height differences between transferred and non-transferred CL.	23
4.11	Difference of CCM surface documented with built-in camera and external camera.	24
4.12	High intensity light image of first formula CCM with big area showing cathode (left) and anode (right), from supplier A	25
4.13	High intensity light image of CCM from supplier D.	25
4.14	High intensity light image of CCM from supplier F.	26
4.15	Degree of transfer for CCMs prepared using PFSA membrane, 0.25 mgPt/cm ² cathode loading and 25 cm ² area.	27
4.16	Degree of transfer for CCMs prepared using PFSA membrane, 0.3 mgPt/cm ² cathode loading and 25 cm ² area.	28

4.17	Degree of transfer for CCMs prepared using PFSA membrane, 0.35 mgPt/cm ² cathode loading and 25 cm ² area.	29
4.18	Degree of transfer for CCMs prepared using PFSA membrane, 0.25 mgPt/cm ² cathode loading and 280 cm ² area.	30
4.19	Degree of transfer for CCMs prepared using PFSA membrane, 0.3 mgPt/cm ² cathode loading and 280 cm ² area.	30
4.20	Degree of transfer for CCMs prepared using PFSA membrane, 0.35 mgPt/cm ² cathode loading and 280 cm ² area.	31
4.21	Degree of transfer for CCMs prepared using HC membrane and area of 25 cm ²	32
4.22	Image of decal substrate showing the freckled non-transferred pattern from the anode.	32
4.23	Color defect shown on CL surface after CCM assembly at 180°C.	33
4.24	Color defect shown on decal after CCM assembly at 180°C.	34
4.25	Image of decal transfer for CCM assembled using cellulose/polyester pad.	36
4.26	Upper pressure pad folded during the hot-pressing.	36
4.27	Image of decal transfer for CCM assembled using polyester pad.	37
4.28	Set-up for CCM assembly using cellulose/polyester as sandwich material under the cellulose pad.	38
4.29	Set-up for CCM assembly using polyester pad and metal plate.	38
4.30	Set-up for CCM assembly using two types of silicone pads.	39
4.31	Set-up for CCM assembly using non-reinforced PTFE as sandwich material under the cellulose pad.	39
4.32	Set-up for CCM assembly using non-residual paper as sandwich material under the cellulose pad.	40
4.33	Illustration of resulting polarization and resistance curves from in-situ testing.	40

List of Tables

5.1	Optimal transfer parameters.	43
-----	--------------------------------------	----

1

Introduction

This chapter serves to introduce fuel cells and the importance of this research topic, along with a clarification of the objectives of this thesis.

1.1 Background

In the advent of climate change there have been increasing pressure to find more sustainable energy sources and energy conversion technologies. In regard to this, more and more attention has been focused on the proton exchange membrane fuel cell (PEMFC) system [1]. There are many reasons for this increased interest in PEMFC, with one being its versatility in generating power for different applications, such as for marine, off/on-road, and aviation. Although perhaps the biggest appeal is its ability to convert energy stored in hydrogen gas into electricity, with only heat and water as by-products. However, a lot of research is still needed in order to optimise both the production and operation of the fuel cell. One of the biggest hurdles to be overcome can be found in what is often described as the heart of the fuel cell, namely the membrane electrode assembly (MEA) [2]. Here is where the electricity is produced by the oxygen reduction reaction (ORR) and hydrogen oxidation reaction (HOR) [3]. This makes MEA a key component of the fuel cell and one way of producing it is the decal transfer method. This method is used to create a 3-layered MEA, also called the catalyst coated membrane (CCM), and will be the topic investigated in this thesis. When using this method temperature, pressure, and time are some of the essential parameters to be considered. However there are other important factors that needs to be investigated such as the type of decal material, type of pressing material and effects of impurities. These are some of the factors that will be considered in this thesis.

1.2 Objective

The objective of this project is to combine literature studies with laboratory work to investigate an efficient and reliable CCM assembly. After completion, the work is expected to generate a better understanding of the following statements and questions:

- Optimizing the transfer parameters for different membranes
- Optimizing the transfer parameters for high and low loading electrodes
- Optimizing the transfer parameters for increased CCM area

- Finding an efficient quality check method
- Investigation of effect of pressing materials
- Comparing quality of in-house CCMs with commercial CCMs, based on pre-defined quality parameters
- Investigation of effect of different decal materials on the quality of CCM

1.3 Importance to Powercell

Powercell has a goal of being able to produce the MEAs needed for their fuel cells in-house. However, there is still more research needed before Powercell can get a fast and reliable production up and running. Previous work, by S. A. Ogu-Egege and D. Schulz, have focused on creating a generalised method for producing the MEAs and on gaining a better understanding of how the different parameters during the hot-pressing affects the MEA [4, 5]. Although these works were of great help at Powercell, there are still many aspects of the assembly that need further investigation and it is therefore this thesis intention of filling some of those gaps of knowledge. The effect of decal used during the decal transfer method will be investigated since it plays a crucial yet not fully understood role in the success of transfer and surface structure of the produced CCM. The work of S. A. Ogu-Egege introduced the use of a pressing material which distributes the pressure evenly across the CCM area and thereby increasing the transfer rate. However, this material has a tendency to leave residues on the CCM, which could negatively affect its performance and it is therefore in the interest of Powercell to replace the pressing material with something that does not leave any residues. In the work by D. Schulz it was explored if it is possible to create multiple CCMs simultaneously by stacking them in the press. This was investigated as it would mean that less time and energy is required for each CCM. Expanding on this reasoning it would therefore also be of interest to Powercell to increase the area of the produced CCM, as the CCM can be cut into smaller ones after the hot-press. The transfer parameters for higher cathode loadings will also be investigated as the loadings of each fuel cell needs to be tailored according to its application, where for example a fuel cell used for aviation would require a higher loading. Another aspect of the thesis is to optimise the transfer parameters for both PFSA and hydrocarbon (HC) membranes. This is of importance since PFSA is the membrane typically used, however the material is not considered environmentally friendly and there is therefore a desire to phase out PFSA and here the HC membrane has emerged as a likely candidate. HC is not only more environmentally friendly, but has in some cases also shown to increase the performance. Finally the thesis will also look into the use of different analytical techniques for relating the quality of the CCMs. This is of imperative importance since the quality of the CCM has a huge impact on the performance and life-time of the fuel cell and Powercell needs to be able to verify the quality of their in-house made CCMs.

2

Theory

This chapter is meant to provide a theoretical background on the inner workings of fuel cells and of its different parts, with a focus on the membrane electrode assembly, which will be discussed and used in this thesis.

2.1 Proton Exchange Membrane Fuel Cell

One of the more common types of fuel cell is the proton exchange membrane fuel cell, also known as PEMFC. A main difference between the PEMFC and other fuel cell types, such as the Solid Oxide Fuel Cell (SOFC), is that the SOFC has oxygen ions traveling through its membrane, while in the PEMFC it is hydrogen ions being transported through the membrane [6]. There are other differences in terms of operating temperature, materials and fuels that can be used, however the PEMFC is the focus of this thesis and a deeper dive into other types is therefore deemed unnecessary.

For the PEMFC, it can use different fuels with some being methanol and biogas, however the most common fuel is hydrogen and air. In the cell the hydrogen and air are used separately and the electricity is gained through two half-cell reactions, see Equation 2.1 and 2.2, giving the overall reaction seen in Equation 2.3.



Figure 2.1 illustrates the fuel delivery and subsequent reactions taking place in the fuel cell. Here the hydrogen flows to the anode side of the membrane and the hydrogen oxidation reaction occurs (HOR), producing hydrogen ions and electrons. The electrons travel through an external circuit, providing electricity to a load, before arriving at the cathode side of the membrane. At the same time the hydrogen ions have traveled through the membrane to the cathode side. Here the oxygen reduction reaction (ORR) between the hydrogen ions, electrons and the flowing oxygen occurs, creating water and heat. The excess water and heat then diffuses out of the cell through the porous structure of the gas diffusion layer (GDL).

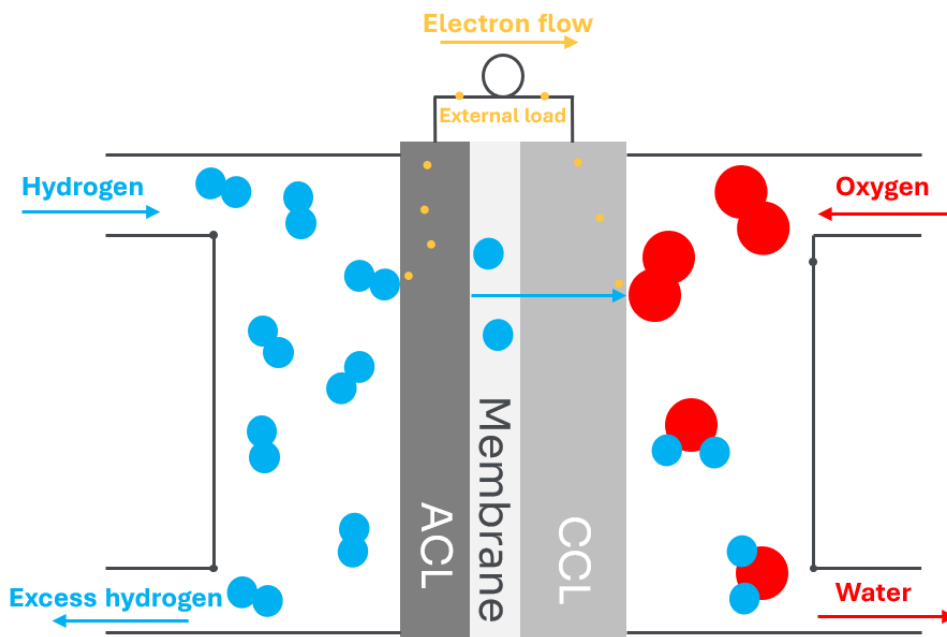


Figure 2.1: Illustration of the flows and reactions occurring in the PEMFC.

2.2 Membrane Electrode Assembly

Membrane electrode assembly (MEA) is considered the heart of the cell as this is where the reactions take place and energy is produced [7]. The MEA in turn, consists of multiple layers with the catalyst coated membrane (CCM), also known as a 3-layered MEA, at its core. The three layers of the CCM is a membrane that is coated with an anode and cathode on either side. Some of the ways to achieve this are by directly spraying the catalyst layer onto the membrane or onto the GDL or it can first be applied to a decal substrate before being transferred to the membrane. The latter is called decal transfer method and is the method used at Powercell and for this thesis. The decal transfer method consists of first preparing the electrodes by coating the catalyst ink onto a decal substrate and letting it dry [3]. Here the thickness of the coating can be varied as a thicker cathode is usually desired to accommodate for the slow oxygen reduction reaction (ORR). The electrodes are then laminated onto the membrane using a hot-press, after which the decal substrates are peeled off, leaving the CCM. The CCM is then expanded upon by adding a sub-gasket on each electrode, resulting in the 5-layered MEA. Lastly, a gas diffusion layer is added to create the seven layer MEA. However three-layered MEA, or CCM, is the type that will be dealt with the most in this thesis.

2.3 Materials of MEA

This section will provide insight into the different materials used in the MEA and its assembly.

2.3.1 Proton exchange membrane

At the center of the CCM is the ionomer membrane, which is used to transport protons from the anode to the cathode side of the CCM. Moreover, it also functions as a physical barrier, impeding the passage of reacting gases and liquids to prevent short-circuiting of the cell [8]. The structure of the most common membranes consists of two parts, one hydrophilic and the other hydrophobic. The hydrophilic part can absorb water allowing it to conduct protons across the membrane, hence the name proton exchange membrane. Traditionally the material used for the membrane has been Nafion, which is composed of a polytetrafluoroethylene backbone with sulfonic acid side-chains [9]. There are many advantages of using this material, such as its high proton conductivity and mechanical properties [10]. However its high price, high gas permeability and decreased ionic conductivity at elevated temperatures has lead researchers to try and find alternative materials that can mitigate these issues [11]. Attempts at phasing out PFAS materials such as PTFE, are also due to their environmental and human impact. Although PFAS is a very large class of materials, with an estimate of over 600 currently used in commercial applications, continuing research reveals a trend of toxicology and bioaccumulation [12], which has led to the European Union declaring their intent to ban the usage of such materials [13]. To stay ahead of the future ban it is therefore of vital importance for the industry to find suitable replacements. To achieve this, a class of materials that has gained attention are the hydrocarbon-based membranes, with polyether ether ketone (PEEK) and polyimide among them. These materials has exhibited good conductivity, thermal stability and low gas permeability. However research is still required to optimize the assembly using this type of membrane.

2.3.2 Catalyst layer

On either side of the previously described membrane is a catalyst layer acting as the electrodes and that usually consists of platinum, carbon black, and ionomer. These components acts as catalyst, support and electrical conductor, and binder and protonic conductor respectively [10]. The structure and composition of these is of importance in order to maximise the CL usage, which is necessary due to the high price of the platinum catalyst. Maximisation is achieved by increasing the number of active sites of platinum catalyst, which can be found at the triple-phase boundary (TPB). The TPB got its name from the three necessary components, for the ORR and HOR, arriving in three different phases to this spot. The electrons are transported through the carbon support in the CL, the protons through the ionomer in the CL, and the gaseous reactants by diffusion through the porous structure. More about the different properties and quality parameters of the catalyst layer can be found in section 2.4.

2.3.3 Gas diffusion layer

The gas diffusion layer is the outermost layer in a 7-layered MEA and its function is to provide a pathway to and from the catalyst layer for the reactant gases and

produced water [2]. This is an important part of the MEA since it ensures that the reactant gases get evenly distributed across the catalyst layer and that the produced water does not accumulate and flood the catalyst layer. This means that the GDL needs to be porous to transport the gases, but it also needs to be thermally and electrically conductive. It needs to be thermally conductive in order to allow the heat generated from the reactions at the catalyst layer to diffuse out from the MEA and electrically conductive to transport electrons to and from the catalyst layer. Regarding mechanical properties the GDL should be flexible enough to provide a good contact angle towards the catalyst layer, but still a bit rigid as to give a measure of stability to the MEA. These requirements can be met by a variety of materials, with some commonly used being carbon paper or non-woven carbon fibers combined with a micro-porous layer [8].

2.3.4 Decal substrates

As the name suggests this is a material that is used during the decal transfer process of the MEA, however it is not a part of the actual MEA and is therefore removed after the process. This usage of the substrate means that it needs to fulfil some specific requirements, these being: adequate adhesion between catalyst ink and substrate as to not cause the dried electrode to flake of, but the adhesion can not be too great as the substrate needs to be peeled of after the hot-press. The substrate also needs to be inert as it can not react with the electrode at any time during the transfer process [7]. It should also ideally not leave any residues or imprints on the resulting electrode after the pressing. Some materials used to try and meet these requirements are PTFE, reinforced PTFE, Teflon and Kapton.

2.3.5 Pressure distribution pads

Pressure pads are used during the hot-pressing to distribute the pressure from the hot-press across the CCM. This practice is based on previous work by S. A. Ogu-Egege, where it became apparent that it is important to get an even distribution of the pressure during the pressing [4]. Non-uniform pressing could lead to decreased yield in transfer of the CL from the decal to the membrane and a less optimal structure of the catalyst layer. Previously a pressure pad of cellulose has been used, however this pad is prone to deposit residues during the hot-press and it is uncertain how or if these residues affects the quality of the CCM. It is therefore of interest to evaluate this and also to test other pressure pads that may not deposit any residues.

2.4 CCM Quality Parameters

The following section is used to explain the different parameters and properties of the CCM that affects its quality.

2.4.1 Porosity and pore-size distribution

One important property of the CCM is the porosity since, as mentioned in section 2.3.2, a porous structure is important to facilitate the transport of reactant gases, but also to expel excess water [3]. In this the pore-size distribution has proven to have a significant role, where a broad distribution is desired [10]. It was reported that a distribution below 25 μm provides fast water removal, while pores above 25 μm are more prone to collect water and flood [14]. Flooding in turn will decrease the performance of the catalyst layer by increasing the resistance of the gas diffusion to active sites.

2.4.2 Thickness

Another parameter is the thickness, where it is important to consider both the catalyst layer and membrane thickness. With regards to the catalyst layer it is of importance since platinum is an expensive material and its utilization therefore needs to be optimal. For example, it is usually desired to have a thicker layer on the cathode side to accommodate for the slow oxygen reduction reaction occurring here. Although it should not be too thick as it would increase the electronic resistance of the catalyst layer and therefore lower the performance [15]. The thickness of the membrane is important for several reasons, one of which is that it lends some mechanical strength to the CCM, meaning that a thinner membrane would in that sense weaken the CCM [16]. On the other hand if the membrane is too thick then this would increase the ionic resistance for the proton transport. Another detail of note is the combination of thickness regarding the catalyst layer and the membrane. This is important since for example a thicker catalyst layer and a thinner membrane can be more prone to forming pinholes [17]. This occurs since the thicker catalyst layer means that more reactions will occur and therefore also more heat. Depending on the thermal stability of the membrane, this extra heat could then degrade the weaker membrane.

2.4.3 Homogeneity

Homogeneity affects the utilization of the catalyst as it influences the number of active sites. A homogeneous and uniform surface of the catalyst layer is desired to increase the number of active sites, but also to make sure that the ionomer is uniformly distributed across the layer, thereby maximizing its usage [8]. A non-uniform layer on the other hand, would lead to inconsistent contact with the GDL causing an increase in electronic/contact resistance and cause areas of high and low conductivity of the catalyst layer [17]. This decreases the performance of the MEA and could create hot-spots. Another drawback is that as the catalyst layer moves during usage the inconsistent contact with the GDL will lead to localised stress concentrations. These localised stresses can then lead to the formation and propagation of cracks through the catalyst layer.

2.4.4 Cracks

Cracks have a dual impact on the quality of the CCM as they can have both a positive and a negative impact. The positive impact works similarly to the porous structure of the layer as they can enhance the mass transportation of the catalyst layer [10, 7, 18]. However it is generally viewed that the negative impacts heavily outweigh the positive. One of the negative impacts is that cracks are often areas of increased localised stress, which can lead to further propagation and formation of pinholes [14, 18]. The cracks also disrupts the structure of the layer, thereby decreasing the electrical contact and increasing the resistance. Cracks are also an area that is prone to accumulate water, resulting in the flooding of nearby pores and increase in mass transport resistance. The flooding and movement of water towards the exposed inner structure also increases the risk of erosion [8].

2.4.5 Delamination

In this case delamination refers to when the electrodes loosen from the membrane and creates pockets of air to form at the membrane-catalyst layer interface. Why this is important to avoid is because these pockets can easily be filled with excess water and just as for cracks this water will the flood nearby pores, causing an increase in mass transport resistance [17, 19]. Additionally the structure of the delaminated catalyst layer is often weaker and more prone to suffer erosion, caused by the flooded water. The decreased contact with the membrane also increases the contact resistance, which means that the proton conductivity from the membrane to the active sites is decreased [20].

During the CCM assembly delamination can occur due to wrinkles in the decal causing voids or because of contaminants between the membrane and electrode [17]. These contaminants could withstand the applied pressure and heat in the press, thereby creating an obstacle that prevents the membrane and electrode to properly adhere at this spot. This decreased adhesion can then cause delamination.

2.4.6 Missing catalyst layer and pinholes

Missing or thin catalyst layer and pinholes primarily affect the quality as they facilitate hydrogen crossover from the anode to the cathode side [21, 22]. Missing CL leads to increase in hydrogen crossover as they are areas of decreased mass transport resistance and hydrogen can thereby reach and diffuse across the membrane more freely. Pinholes refers to defects where there is not only missing CL but also a hole through the membrane, which means that the hydrogen can cross without any major hindrance. This will cause short-circuiting of the cell and lower the net-voltage. The rate of this crossover has a major impact on both the performance and lifetime of the fuel cell [8]. When it comes to missing and thin catalyst layer spots they can also be areas of increased stress concentrations, often resulting in the nucleation of cracks at the borders of the affected area.

Areas of missing or thin catalyst layer are often caused by incomplete transfer from the decal to the membrane, as some of the catalyst layer is still stuck on the decal [14]. Pinholes are most often present before CCM assembly, but could also occur due to contaminants at the membrane-catalyst layer interface [23]. If this contaminant is able to remain rigid and hard at the higher temperature of the hot-press, then it is most likely harder than the membrane and can thereby penetrate the membrane during the high pressure of the hot-press.

2.5 Analytical Techniques

This section serves to explain the basis of the analytical techniques used, along with how and why they were used for the purpose of this thesis.

2.5.1 Optical microscope

Often also referred to as light microscope, this technique uses visible light to show magnified images of smaller objects through a lens [24, 25]. Optical microscopes have been widely used in research for a long time, with perhaps some of its biggest upside being that it is easily set-up and operated and that little to no sample preparation is needed. The most simple optical microscope uses an eye-piece from which the magnified object can be seen, while more advanced ones can show the images directly on a computer screen, where pictures can be taken of areas of interest. The microscope used for this thesis was the Leica DVM6 microscope.

Another advantage of the optical microscope is that it is a non-destructive technique (NDT) when it comes to analysing surfaces of the sample. However there are also drawbacks, such as its limitations regarding low resolution and that the sample needs to be cut/damaged to get a cross-section if the subsurface is to be analysed.

2.5.2 Light board

This is a board with a built-in light across its surface, which allows for back-lighting of the CCM. The CCM is laid down on the board and the back-lighting is then supposed to show defects such as cracks and holes in the CCM as white spots.

2.5.3 High intensity light

This is a device that has been developed internally at Powercell, which means that a detailed description can not be given due to confidentiality. However, the basic principle of the technique is that a high intensity light is able to show defects and pinholes in the CCM, as they will show as bright spots.

2.5.4 In-situ testing

In-situ testing is a common way of evaluating both the performance and resistance properties of a MEA. The performance is evaluated by measuring the cell voltage

as the current density is varied, with the measured data resulting in a so called polarization curve, see Figure 2.2. This curve can then be divided into three different regions, namely the kinetic, ohmic, and mass transport region, where each region is characterised by the phenomenon causing losses in cell voltage. Another point of interest in the curve is the open circuit voltage (OCV).

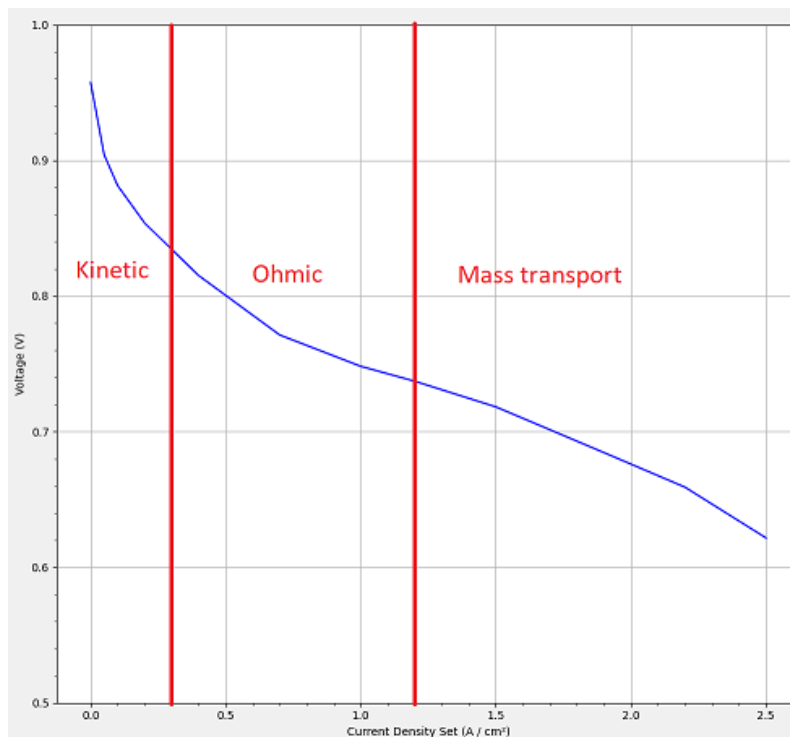


Figure 2.2: Illustration of the different regions in a polarization curve.

The OCV is the voltage measured at the beginning of the curve and gives a direct indication of any presence of leakage or of pinholes. A theoretical cell under standard conditions would have an OCV of 1.23 V, however this is not the case in real life as there is always some hydrogen crossover occurring and the measured OCV is therefore always lower than 1.23 V. A well-functioning and pristine cell should exhibit an OCV above 0.9, where a lower OCV would indicate greater amount of leakage. If the OCV goes below even 0.8 V then this would indicate the presence of a pinhole.

The first region of the curve is the kinetic region, where the voltage loss is mainly attributed to the reaction kinetics of the cell. More specifically, since the hydrogen oxidation reaction (HOR) is a relatively fast reaction, it is the oxygen reduction reaction (ORR) that has the biggest impact. In the second region, called the ohmic region, the dominating factor for the voltage losses is the resistance to the flow of electrons and protons. Due to the electrons superior flow-characteristics it is mainly the resistance to conduction of protons that gives rise to the losses. This resistance primarily stems from the membrane and membrane-electrode interface. The third

and last region is the mass transport region and as the name suggests, the limiting factor here is the mass transport within the cell. In this region the voltage losses primarily occur on the cathode side, since the diffusion of oxygen here is much slower than the hydrogen diffusion at the anode. A point of interest in this region is the full-load point, which can be found at a current density of 2.5 A/cm^2 . This point gives an indication of the quality of the MEA, where 0.6 V is considered the tipping point between a good and bad MEA.

3

Methods

The methodology for the thesis consisted of preparing and evaluating the 3-layered CCM. Assembly of the CCM was done using the decal transfer method, see section 3.1, and different parameters of the assembly were examined to get a better understanding of how and what affects the quality of the CCM. A comparison of the quality between in-house and commercial CCMs was also conducted. Previously at Powercell the only quality check method used was with a light board, which was deemed insufficient, and therefore other methods of quality control were investigated in this thesis.

3.1 Decal Transfer Method

As previously explained in section 2.2, the CCMs in this thesis were prepared using the decal transfer method. Although that only served to provide a general and brief explanation of the method and this section will therefore dive deeper into the method and explain how it was used specifically for this thesis.

Firstly, a cathode and an anode coated onto a decal substrate was required and for this thesis the electrodes were both commercial and in-house made. The in-house electrodes were prepared by another employee at Powercell, following requested specification in terms of loading and decal substrate. The prepared electrodes were then checked with a light board and high intensity light to detect defects and areas that should not be used. A pre-shape for the CCM was then cut out of the electrode, in the shape of a 6x6 cm square. This was also done with the membrane, which was always a commercial one. The electrodes were then placed on top of each-other, with the decal facing outwards and the membrane in between. This was then placed in a cutter that was used to get a specific shape of the CCM with a 5x5 cm size. After this, two 6x6 cm squares of the pressing material were cut and the CCM was placed between the two pads. The pressing material was made slightly larger to ensure that the entire CCM was covered.

The CCM was then loaded into the hot-press and pressed using the temperature, time, and pressure specified for that particular CCM. When the hot-press was complete, the CCM was retrieved and the decals were peeled off to get the finished CCM. The decals were peeled immediately after removing the CCM from the hot-press, to prevent the material from cooling too much.

3.2 Comparison of Analytical Techniques

In order to get a better understanding of how the important properties and qualities of the CCM can be investigated, the light board, high intensity light, and optical microscope, introduced in section 2.5, were used to study the CCMs and then compared to one another. This was also done with the intention of being able to justify the selection of one or more techniques for further use as tools for quality control. Properties of the techniques that were compared include: time, cost, ease of analysis and if sample preparation is needed. However, more importantly the technique's ability to identify important properties and defects of the CCM was assessed.

The light board had been used previously at Powercell and its usage is straightforward, as the electrode or CCM is placed upon the board for analysis. The light is then turned to the brightest setting and documentation is done by either marking the sample or capturing an image of the sample with an external camera. It was a bit different for the high intensity light, since this was a newer tool at Powercell and it did not have any standardised usage or settings. Optimization, such as the intensity of light, whether to capture images in the dark or light, and from which side of the CCM the image should be taken, therefore had to be done before the technique could be compared to the others. Similarly to the high intensity light, the microscope did not have any standardized settings for analysing the CCMs and initial time therefore had to be spent in getting to know the technique and the different settings, such as which optical lens, magnification, and colour-scheme should be used.

3.3 Commercial CCM Quality

The quality of commercial CCMs acquired by Powercell were examined using light board, high intensity light, and optical microscope. This was done to enable comparison of the commercial CCMs with in-house CCMs, in terms of quality and appearance. The manner and extent to which the different analytical tools were to be used for this quality check depended on the outcome of the investigation detail in the previous section.

3.4 Experimental Matrix for Optimization of Transfer Parameters

Initial experiments were conducted to optimise the transfer parameters for the decal transfer method when three different loadings, a smaller and a bigger CCM area and two different membranes are used. The definition of optimised is in this case considered to be when a complete transfer has been achieved on both electrode sides. To manage this an experimental matrix, which was the same for both membranes,

3.6 In-situ Testing

In order to perform the in-situ testing, MEAs had to be assembled using the prepared CCMs. To do so, sub-gaskets were cut with a plotter cutter and laminated along the edges of the CCM to properly seal it. After this 5x5 cm squares of the GDL were cut and added to create the finished MEA. One MEA at the time was then loaded into a single cell set-up and conditioned for 12 hours to prepare it for the testing procedure. The testing was then performed under normal operating conditions with a relative humidity of 60%, cell temperature of 65°C, and reactant flow in excess by a factor of 5 and 6 to the anode and cathode respectively. During the testing, a total of three polarization curves was run for each MEA and the mean value of these was used for the analysis.

4

Results

4.1 Comparison of Analytical Techniques

The following chapter will detail the results given by the different analytical techniques and use these to compare them to one another.

4.1.1 Light board

The light board, as explained in section 2.5.2, was evaluated to see if it can be used to detect defects such as holes and cracks in the CCM. The three first CCMs produced, as seen on the light board in Figure 4.1, showed no visible defects. This would indicate that all three CCMs were homogeneous and free of defects, however, as seen in section 4.1.2, the high intensity light showed that there were indeed defects in CCM 1. This means that the high intensity light can be used to detect defects that are not visible with the light board and the ability of the light board to detect defects was therefore questioned.



Figure 4.1: Analysis of CCM 1, 2 and 3 using the light board.

Although, further usage showed that the light board was able to detect defects, albeit much bigger defects than those detected with the high intensity light. Figure 4.2 shows an analysis of an anode before the assembly of the CCM. For this anode several large holes can be seen and these areas could then be marked and avoided when cutting pieces for the CCM.



Figure 4.2: Analysis of anode for usage in CCM assembly, using the light board.

Figure 4.3 shows the fifth CCM, which only had some transfer, and here a lot of defects can be seen in the CCM. That these were visible with the light board was likely due to the poor transfer, the size of the defects and the missing catalyst layer. Although this did indicate that the light board can detect defects, it also showed that the sensitivity is low compared to the high intensity light and that the light board might not be the best tool for analysing the quality of the assembled CCMs. If it is to be used then it would work best to indicate areas of electrodes that should be avoided in the assembly, such as the ones seen in Figure 4.2.

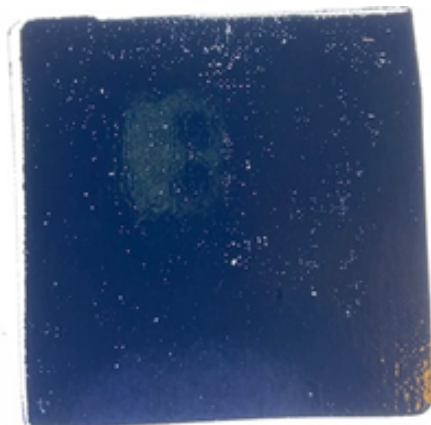


Figure 4.3: Analysis of CCM 5 using the light board.

4.1.2 High intensity light

Although the high intensity light works a bit differently to the light board, see section 2.5.3, they were both planned to be used for detecting similar defects of the CCM. As previously explained in section 4.1.1, the initial study of the three first CCMs assembled showed that the high intensity light could not only detect defects, but it also had a better sensitivity than the light board, see Figure 4.4.

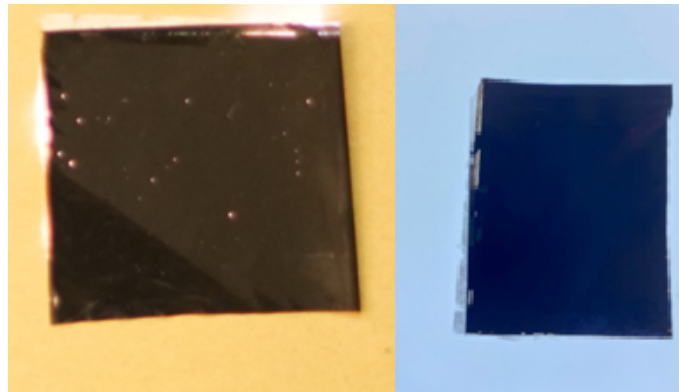


Figure 4.4: Images comparing CCM 1 using high intensity light and light board respectively.

However before further use, the technique needed to be optimized. To start with the intensity of the flash was altered to see if the observed defects varied with it. Based on these results and the thought that a too strong flash might affect the integrity of the CCM (TRUE?) an intensity of 1/16 was chosen.

It was also investigated whether images should be taken in the dark or light, where images were taken of multiple CCMs in both environments. The results showed that more defects could be seen for images taken in the light, see Figure 4.5, however this was believed to be caused by the reflection of light and not actually defects of the CCM. To avoid falsely observing defects it was therefore decided to use the high intensity light in the dark.



Figure 4.5: Images comparing CCM 14 in dark (left) and light (right).

After this the difference in observed defects depending on which electrode side was placed face-up was investigated. To do so images of the CCMs with both sides up was captured and compared. It was observed that some CCMs exhibited different defects depending on which electrode was face-up and although it was, at the time, unclear as to why this was the case it was still decided that both sides were to be used in the work. This was decided with the hope that comparison of the two sides

4. Results

could aid in the determination of what defects were shown in the high intensity light images.

Even after these alterations there were still a few drawbacks observed for the high intensity light. One of which was its inability to show an area of incomplete transfer, however these can be seen clearly with the naked eye. Another drawback was the need to have the CCM resting on the edges of the hole as this meant some defects on the edges of the CCM might have been blocked from being illuminated by the flash. There was also the difficulty in identifying the nature of the defects, as in whether it is missing CL on one or both side of the CCM or a pinhole through it. As mentioned earlier, images were taken from both sides of the CCM in an attempt to compare them and identify pinholes. However even if two shown defects align on both sides it can still not be declared a pinhole based on the high intensity light alone, as that would require a hole through the membrane. Another idea that was tried was to take images of the electrodes before they were used and then correlate the used area of the electrode to its corresponding CCM, see Figure 4.6. The intent was to evaluate if already existing defects on the electrodes could be seen on the finished CCM or if the CCM showed new defects that might have occurred during the transfer process. It was also done with the hope of relating the grade of transfer to the quality of the original electrode. This was found to be particularly difficult for the cathodes as the areas used were difficult to distinguish from one another and their impact could therefore not be related. It was somewhat easier for the anodes, as these generally showed fewer and bigger defects differentiating the used areas. However, a clear trend between size or number of defects on the anode relating to the rate of transfer could not be found.



Figure 4.6: Illustration of areas used from the cathode (left) and anode (right) during the assembly and their corresponding CCM.

Another attempt in clarifying the defects shown was made by a one-sided assembly, which means that one electrode at a time was transferred to the membrane and images taken at each step, see Figure 4.7. This was done to evaluate how each added component of the CCM affects the defects shown. First an anode with a big and small missing CL defect was chosen and evaluated with the intense light. The anode was then transferred to the membrane and another image was taken. This showed that the membrane has no effect on the clarity or intensity of the anode defects shown. After this the cathode was transferred and the full CCM evaluated.

This time the smaller missing CL defect could no longer be seen and the bigger one could only be seen as very small dots. However, missing CL defects of this size would normally be avoided during the CCM assembly and only defects such as the smaller one might be present on the anodes used. The visible dots on the finished CCM were believed to be caused by aligned missing CL on the cathode side.

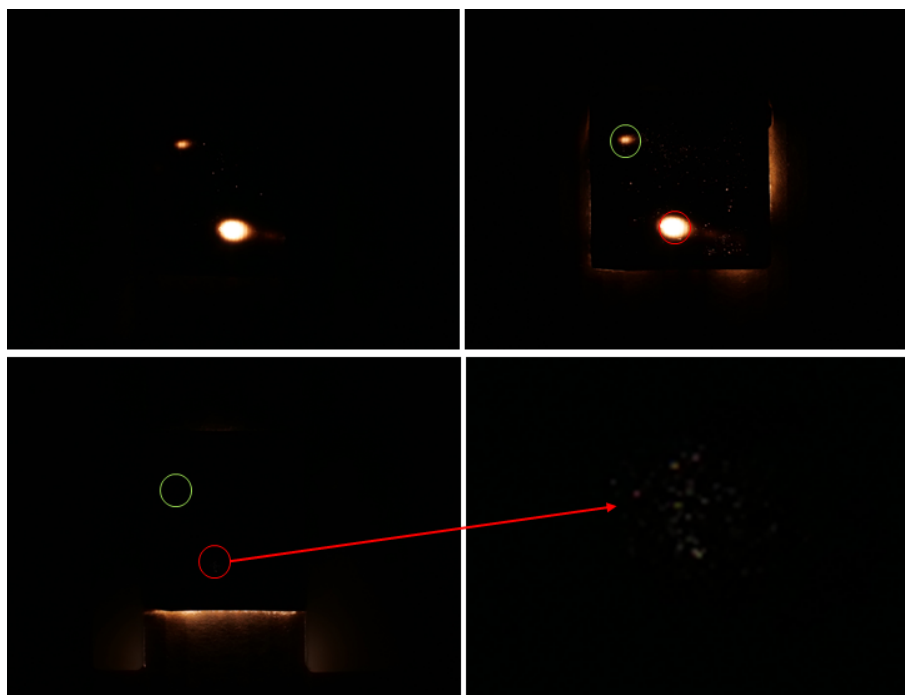


Figure 4.7: High intensity light images during the stages of one-sided assembly: bare anode (top left), anode transferred to membrane (top right), full CCM (bottom left) and focus on defect (bottom right). The green and red rings mark two areas of missing catalyst layer on the anode.

Lastly, an artificial pinhole was added to the CCM and evaluated, see Figure 4.8, which showed that the pinhole was clearly visible from both sides of the CCM and that it was much more visible than the missing CL defect. These results suggested that only pinholes or missing CL defects aligned on both sides of the membrane are visible using the high intensity light.

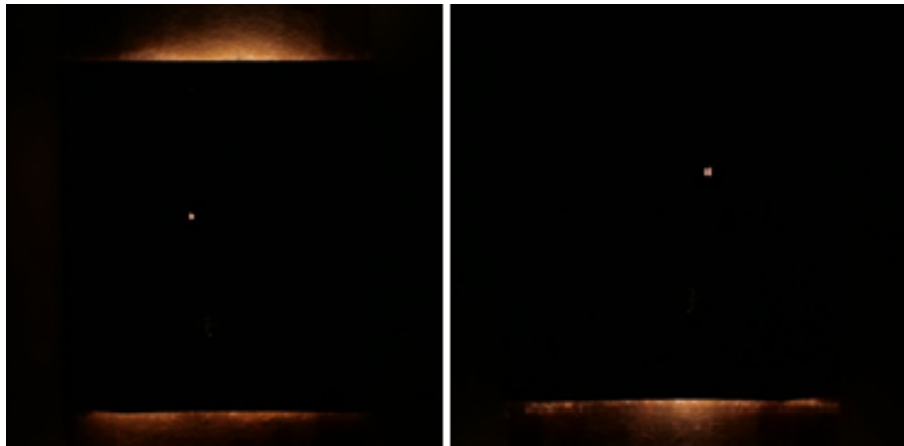


Figure 4.8: High intensity light image of CCM with artificially added pinhole, seen from cathode (left) and anode side (right).

From the results detailed above, one conclusion could be that only pinholes and aligned missing CL are visible in the high intensity light. However, pinholes are rarely created during the decal transfer process and missing CL spots are quite unlikely to fully align. It was therefore proposed that even missing CL that are only partly aligned or in near proximity can be seen. This would broaden the number of defects visible with this method, see Figure 4.9, and explain why so many defects could be seen for some of the CCMs. Although further investigation is still required to fully understand to which extent these additional defects can be seen.

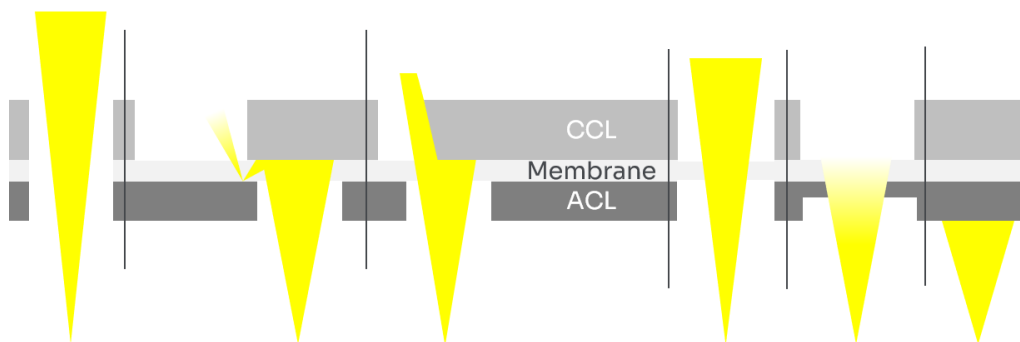


Figure 4.9: Illustration showing how the light passes through the CCM in the case of: pinhole, missing CL in close proximity, partly aligned missing CL, aligned missing CL, missing CCL and thinner ACL, and lastly non-defected CCM.

4.1.3 Optical microscope

The optical microscope was used because earlier work at Powercell had proved it capable of analysis of defects such as cracks, holes and scratches. It was therefore of interest to evaluate its efficiency as a quality check tool during CCM assembly. What became quickly apparent was that it required significantly more analysis time, compared to both the light board and high intensity light, and the defects shown

relied a lot on the settings used and competence of the analyst. There was no standard set for how the CCMs were to be analysed using the microscope, which meant that the settings were varied each time to try and get the best image possible of the CCM. This in turn meant that even the same CCM was likely to appear different between each analysis and comparison between different CCMs was thereby made more difficult. Another drawback was the difficulty of finding unknown defects using only the microscope. The built-in back-lighting was often too weak to show holes or aligned missing CL, that for example was shown using the high intensity light, and considerable time was then spent searching across the surface of the CCM for apparent defects. This problem could be somewhat alleviated by first using the high intensity light and then search the area of the shown defect with the microscope. However, even after finding the defect not a lot of further information could be deduced which could be of use in this thesis work. Although some features of interest can be seen in Figure 4.10, where the width of a crack, calculated area of a missing CL spot and height differences in the CCM can be seen. Initially, the width and calculated area features were of interest since an idea was that a trend regarding the extent of defects between complete and almost complete transfer could be found. However, after examination of various CCMs with both levels of transfer no trends regarding the size of miss CL spots could be found. Only a trend of the amount of defects was found, where the completely transferred CCMs rarely showed defects.

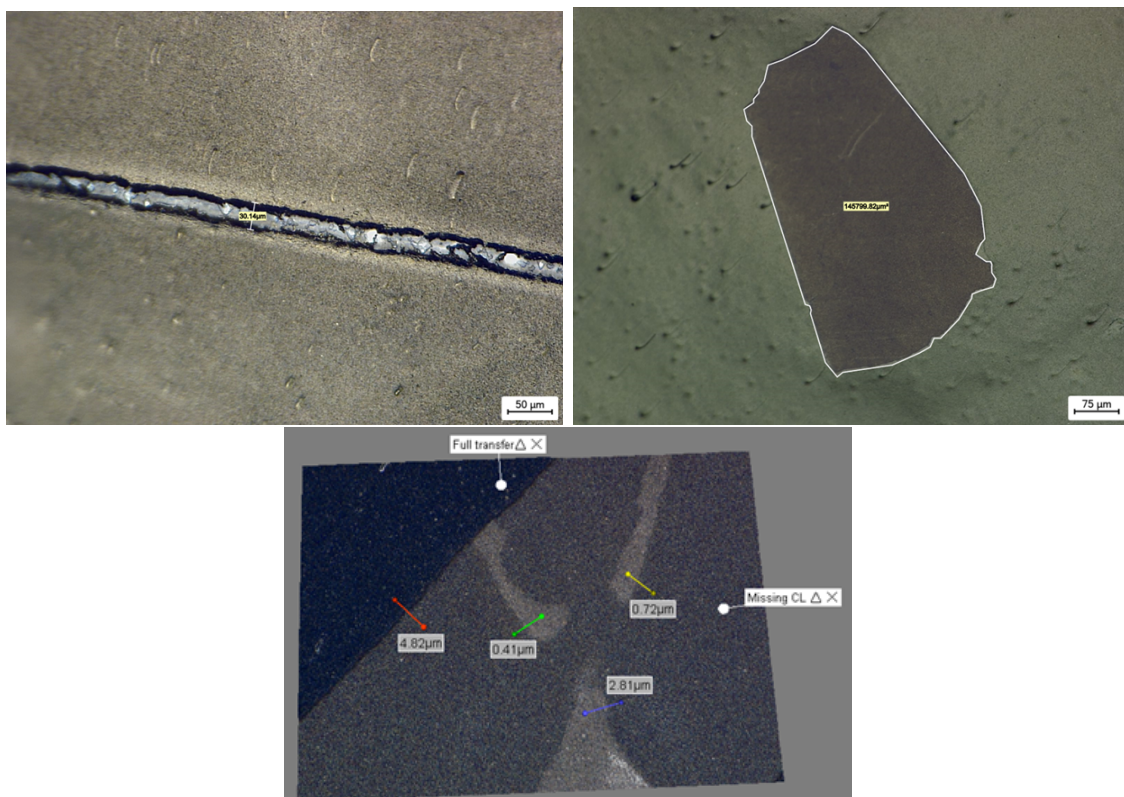


Figure 4.10: Optical images detailing the width of a crack, area of a missing CL, and height differences between transferred and non-transferred CL.

Yet another drawback for the optical microscope is the CCMs tendency to bend onto itself and its sensitivity for light, which made it difficult to document the observed defects with the camera. Figure 4.11 shows the difference of what was seen in the microscope when analysing the CCM and what can be seen in the image taken by the built-in camera.

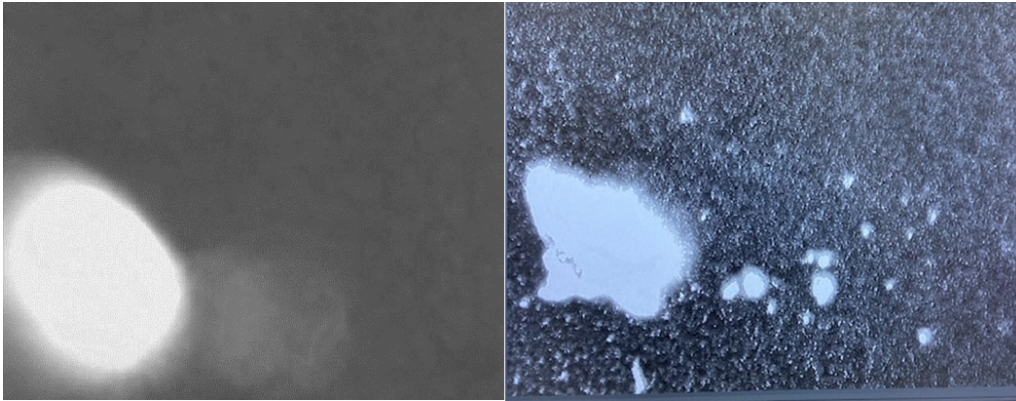


Figure 4.11: Difference of CCM surface documented with built-in camera and external camera.

The extensive operating time required and subsequent lack of additional information given by the optical microscope, means that it is not advised as a quality check method during CCM assembly.

4.2 Commercial Quality Check Using High Intensity Light

As previously explained in the first paragraph of section 4.1.2, the high intensity light proved to be a superior technique for quality check of the CCMs, compared to the light board. For this reason it was deemed unnecessary to use the light board for quality control of the commercial CCMs and the high intensity light was then the only technique used for this purpose. A total of seven different CCM suppliers were analysed and compared.

Three different samples were analysed from supplier A, two of which were of the same CCM formula but with different sizes and the third had a different formula. The first formula gave mixed results in terms of quality as the smaller CCM showed no indication of defects, however the same can not be said for the bigger CCM. As can be seen in Figure 4.12, this one showed multiple defects, both in the form of dots and lines. Given that this is a commercial CCM it is uncertain as to the origin of these defects. They could be due to the assembly process or due to handling, transportation, and storage of the CCM. The second formula of CCM showed no indication of defects.

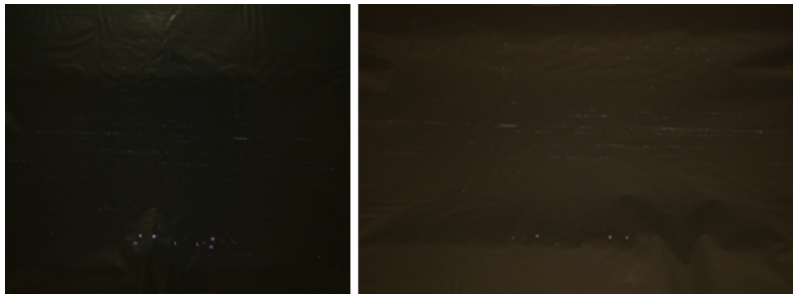


Figure 4.12: High intensity light image of first formula CCM with big area showing cathode (left) and anode (right), from supplier A

Only one sample from each of supplier B and C were checked and indicated that the CCMs had no defects. The sample from supplier D can be seen in Figure 4.13, where the analysis showed a few defects on the CCM. Although there were far less defects on the CCM from supplier D than the one from supplier A.

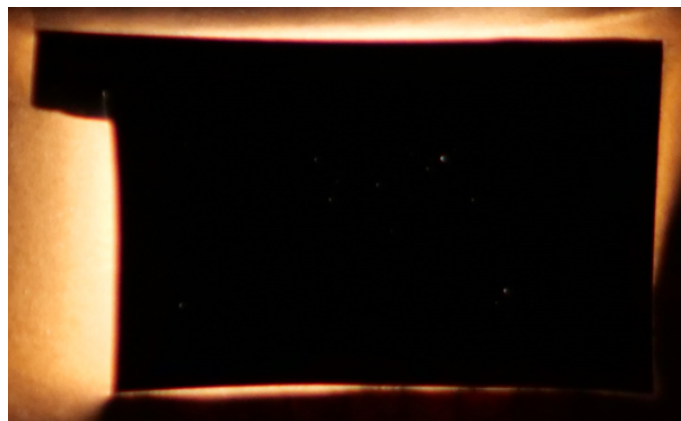


Figure 4.13: High intensity light image of CCM from supplier D.

From supplier E one CCM was analysed and this indicated that the CCM had no defects. The last commercial CCM checked, from supplier F, can be seen in Figure 4.14 and showed the presence of one defect in the CCM. What differentiated this CCM from the other commercial ones was that this hole was only visible when the intensity of the flash was increased from 1/16 to 1/4.



Figure 4.14: High intensity light image of CCM from supplier F.

Apart from the three defected CCMs, the commercial CCMs appeared to be of good quality. The quality was comparable to the CCMs prepared with in-house electrodes for this thesis, when there was a complete transfer of the electrodes, as these also showed no or very few defects in the high intensity light. However, as has been previously discussed in section 4.1.2 not all defects on the original electrodes may appear on the finished CCM. Which means that the commercial CCMs may have defects such as missing CL areas or cracks that are not visible in this analysis.

4.3 Optimization of Transfer Parameters for PFSA Membrane

4.3.1 Low loading and small area

Low loading is in this case referring to 0.25 mgPt/cm^2 and the small area is 25 cm^2 . All CCMs were prepared according to the procedure outlined in section 3.1 and the results can be seen in Figure 4.15. As mentioned earlier each transfer was graded from incomplete to complete transfer and shown in colours from red to dark green. The starting point of 160°C and 300 N/cm^2 was chosen based on earlier work at Powercell, where complete transfer had been achieved with these parameters. However, this work had used different decal and cathode loading and some variation was therefore expected. This was just the case, as only two out of four CCMs had complete transfer and further optimisation was therefore necessary.

The next step was then to increase the pressure to 450 N/cm^2 , which proved to increase the transfer rate as all four CCMs had complete transfer. Another thing of note for these CCMs was the ease of which the decal could be peeled of. Usually some bending of the corners and peeling with tweezers from bubbles formed was required to peel the decals, however when bent half the decal disconnected from the

CCM by itself for these CCMs. The rest could then very easily be peeled off. This could indicate that the desired adhesion between the CL and membrane has been achieved using these parameters.

After this the temperature was increased to 180°C to see if the same transfer could be achieved at an elevated temperature. This appeared to not be the case as one CCM had incomplete transfer and the other three only had some transfer. A rare defect was also visible on each of these CCMs, where the surface structure had changed and some colour shift of a greenish colour could be seen. A more in-depth discussion of what this defect might be is given in Section 4.5. The defect could be seen on the cathode side for the bad transfers and on the anode side for the incomplete transfer. To complete the matrix the pressure was then decreased to the original 300 N/cm². This was also done to see if the combination of increased pressure and temperature might have led to the poor transfer and the rare defects shown in earlier CCMs. However, the transfer was even worse at the lower pressure, with three incomplete transfers and one CCM with some transfer. This could indicate that while the higher temperature decreases the adhesion of CL to membrane, the increased pressure somewhat mitigates this. The poorly transferred showed none of the colouring defect, whereas the incomplete transfers all exhibited the defect on the anode side. This seems to correspond with the previous incomplete transfer, where the rare defect also occurred on the anode side.





0.25 loading - 25cm² - PFSA		
t=300s	Pressure [N/cm²]	
T [C]	300	450
180		
160		

Figure 4.15: Degree of transfer for CCMs prepared using PFSA membrane, 0.25 mgPt/cm² cathode loading and 25 cm² area.

4.3.2 Middle loading and small area

This was intended to be the first matrix to be performed, as it would act as a guideline for within which boundaries a complete transfer was likely to occur, even at other loadings and bigger area. This particular matrix was chosen as the starting point based on its similarity to the loading and area used for previous work. This work found that 160°C and 300 N/cm² was the lowest temperature and pressure where complete transfer was achieved. It was therefore used as the initial parameters for the hot-pressing, to be expanded upon to find the limits of complete transfer. 160°C and 300 N/cm² was the first combination to be examined and had achieved

4. Results

complete transfer, when using a different decal. As can be seen in Figure 4.16, the use of a new decal had major effect on the transfer. Instead of four complete transfers, one almost complete and three with only some transfer occurred. This was not unexpected, given the different properties of the decals, however it did mean that the optimal parameters had to be found before investigating the limits. As with the lower loading, the pressure was then increased to 450 N/cm². Unlike for the lower loading, this time only one complete transfer was achieved and the pressure was therefore further increased to 600 N/cm². All four CCMs at this pressure achieved complete transfer and the optimal parameters was therefore believed to have been found.

To confirm this and to find the investigate the temperature and pressure limits of this particular decal and membrane, the rest of the matrix was finished as well, with the exception of the boxes marked purple. These were not completed since, for example the CCMs assembled at 120 °C and 600 N/cm² showed that this temperature is likely too far away from the T_g of the membrane and will therefore not lead to complete transfer. The CCMs assembled at 160 °C and 50 N/cm² also showed the importance of added pressure and that 50 N/cm² is too low to properly adhere the CL to the membrane. At the elevated temperature of 180 °C the same color defect as for the lower loading was noted on 12 out of 16 of the assembled CCMs and the higher temperature generally lead poor or incomplete transfer, where the ones assembled at 150 N/cm² once again showed the importance of adequate pressure. CCMs assembled at 140 °C showed surprisingly dependable results as they all had roughly the same level of transfer, however none of them had complete transfer and this shows that there is likely only a small window for complete transfers around 160 °C. This would also corroborate with the T_g of the membrane and ionomer being around 160 °C.

0.30 loading - 25cm ² - PFSA					
t=300s	Pressure [N/cm ²]				
T [C]	50	150	300	450	600
180	purple	red	yellow	red	yellow
160	yellow	green	yellow	green	green
140	purple	green	green	green	green
120	purple	purple	purple	purple	green

Figure 4.16: Degree of transfer for CCMs prepared using PFSA membrane, 0.3 mgPt/cm² cathode loading and 25 cm² area.

4.3.3 High loading and small area

The results for the high loading, 0.35 mgPt/cm^2 , can be seen in Figure 4.17. Yet again, the starting point was chosen to be 160°C and 300 N/cm^2 and as with previous loadings this did not lead to complete transfer of the CCMs. The pressure was then increased to 450 N/cm^2 , which led to somewhat better transfer as one CCM was completely transferred. However this does not fill the requirement of all four CCMs being completely transferred. Which is why the pressure was increased once again, this time to 600 N/cm^2 . This led to four completely transferred CCMs and the optimal transfer parameters for this loading had therefore been found.

To finish the matrix and to evaluate if the same color defects occurred for the higher loading, the temperature was then increased to 180°C and CCMs for each of the three pressures were made. As can be seen the overall transfer was worse at the elevated temperature for the higher loading, as well as the occurrence of the color defect on 8 out of 12 CCMs. The trend seen for the lower loading, where increased pressure at the elevated temperature seemed to increase the rate of transfer, can not be seen in this matrix.

		0.35 loading - 25cm ² - PFSA		
t=300s		Pressure [N/cm ²]		
T [C]		300	450	600
180				
160				

Figure 4.17: Degree of transfer for CCMs prepared using PFSA membrane, 0.35 mgPt/cm^2 cathode loading and 25 cm^2 area.

4.3.4 Low loading and large area

The optimised transfer parameters for CCMs with 0.25 mgPt/cm^2 and 25 cm^2 , found in Section 4.3.1, were used as a starting point when evaluating the optimal parameters for a bigger area of 280 cm^2 . This was done since a larger area was not expected to greatly affect the temperature and pressure needed to adhere the electrodes to the membrane. This theory was based on the loadings being the same and that the required energy per cm^2 would therefore remain the same. As can be seen in Figure 4.18, this was also the case as two CCMs at 160°C and 450 N/cm^2 had complete transfer. To further confirm that the CCM area does not influence the optimal parameters, an additional two CCMs were assembled at a lower pressure of 300 N/cm^2 . Neither of these CCMs had complete transfer, thereby indicating that the optimal transfer parameters for the 25 cm^2 and 280 cm^2 CCMs are the same.

0.25 loading - 280cm ² - PFSA		
t=300s	Pressure [N/cm ²]	
T [C]	300	450
160		

Figure 4.18: Degree of transfer for CCMs prepared using PFSA membrane, 0.25 mgPt/cm² cathode loading and 280 cm² area.

4.3.5 Middle loading and large area

The middle loading of 0.3 mgPt/cm² with a smaller area of 25 cm² was found to reliably give complete transfers at 160°C and 600 N/cm² and this was therefore used as the starting point for the larger area as well. Two CCMs were made using these parameters, which both had complete transfer, indicating that the larger area of 280 cm² has the same optimal parameters as the smaller area.

0.3 loading - 280cm ² - PFSA		
t=300s	Pressure [N/cm ²]	
T [C]	600	
180		

Figure 4.19: Degree of transfer for CCMs prepared using PFSA membrane, 0.3 mgPt/cm² cathode loading and 280 cm² area.

4.3.6 High loading and large area

Just as for the low and middle loading, the optimised parameters found for this loading at the small area were used to evaluate the transfer with an increased area. Therefore two CCMs with an area of 280 cm² were prepared at 160°C and 600 N/cm². As can be seen in Figure 4.20, they all had complete transfer, indicating that the optimised parameters for CCMs with 0.35 mgPt/cm² and 280 cm² are the same as for 25 cm².

0.35 loading - 280cm ² - PFSA	
t=300s	Pressure [N/cm ²]
T [C]	600
160	

Figure 4.20: Degree of transfer for CCMs prepared using PFSA membrane, 0.35 mgPt/cm² cathode loading and 280 cm² area.

4.3.7 Comparison between loadings

From previous sections it can be deduced that a higher cathode loading required an increase in pressure for complete transfer. This behaviour is not unexpected since a higher loading means a thicker CCL and therefore more energy or adhesion would be needed to adhere it to the membrane. The middle and higher loading had the same optimal parameters, which could be caused by the decreased accuracy of the cathode loading at higher loadings. This means that the range of actual loadings for the 0.35 mgPt/cm² cathodes are likely closer to the 0.3 mgPt/cm², then 0.3 mgPt/cm² is to 0.25 mgPt/cm² and would therefore have more similar properties for complete transfer. When comparing trends between the loadings its clear to see that they all have the general trend of an increase in pressure leading to a better transfer. Additionally, they all experienced the color defect and worse transfer at 180°C, which gives a clear indication of an upper temperature limit regardless of cathode loading.

4.4 Optimization of Transfer Parameters for HC Membrane

Due to both time-constraints and availability of electrodes, the investigation of optimal transfer parameters when using a HC membrane had to be considerably reduced. When first planning the thesis work it was the intention of making this investigation as extensive as the one for the PFSA membrane, however in the end only 17 CCMs with HC membrane were assembled. The results, as seen in Figure 4.21, shows that for complete transfer with a HC membrane a considerably higher pressure is needed. This is not unexpected since the T_g of the HC membrane is higher than for PFSA, but from the PFSA optimisation it became evident that the decals can not be used above 160 °C. The temperature limit was also confirmed when using HC membrane as a CCM assembled at 180 °C and 600 N/cm² was affected by the color defect. So at the 160 °C used the ionomer in the CL is close to its T_g and softens, however the HC membrane is still significantly under its T_g, meaning it will not soften as much and the adhesion between ionomer and membrane is therefore reduced. The results then indicates that an increased pressure can counteract this reduced adhesion.

4. Results

0.25 loading			0.30 loading			0.35 loading			
Pressure [N/cm ²]			Pressure [N/cm ²]			Pressure [N/cm ²]			
T [C]	450	600	T [C]	750	900	T [C]	600	750	900
160			160			180			
						160			
			140						

Figure 4.21: Degree of transfer for CCMs prepared using HC membrane and an area of 25 cm².

There was also a difference seen in the pattern for the non-completely transferred CCMs when using HC membrane, as opposed to PFSA. This can be seen in Figure 4.22, where the almost completely transferred anodes all left a freckled pattern on the decal. This is an indication of insufficient adhesion obtained between the CL and membrane. The freckled pattern was seen on all three loadings and they each followed the trend of fewer freckles appearing as the pressure was increased, until complete transfer was achieved. Reliable complete transfers, and therefore optimal transfer parameters, was achieved for the 0.3 and 0.35 mgPt/cm² at the same parameters of 160°C and 900 N/cm². Due to lack of electrodes the optimal parameters for the lower loading of 0.25 mgPt/cm² could not be found, but based on the trends shown for the other two loadings these are believed to be at 160°C and 750 N/cm², although actual assembly would need to be conducted to verify this.

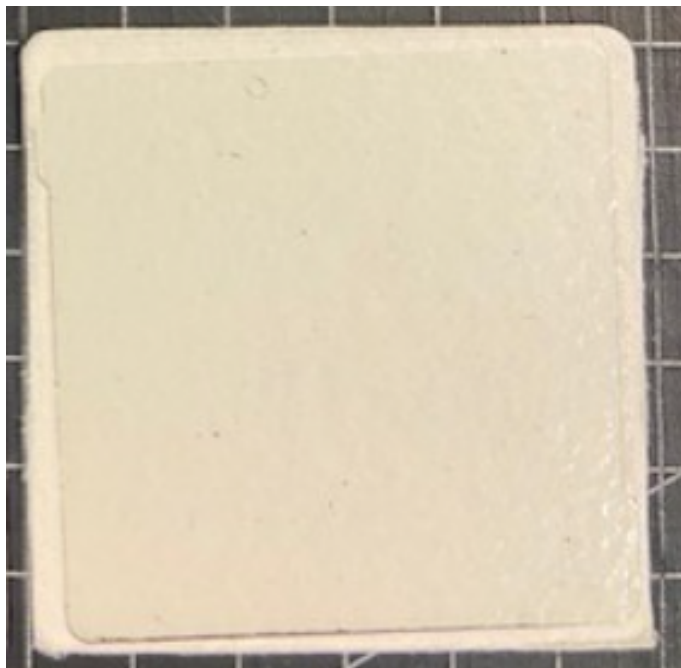


Figure 4.22: Image of decal substrate showing the freckled non-transferred pattern from the anode.

4.5 Investigation of Color Defect

The color defect, first mentioned in section 4.3.1, that was observed at 180°C was something that had not been observed at Powercell before and it was initially unclear what might be the cause of the defect. An investigation was therefore needed to understand what happens at this elevated temperature and what component is affected. It was initially believed that it could be either the decal or the ionomer in the CL that has been affected. This was based on the change of color and roughness at the decal and CL surface, see Figure 4.23. However, the glass transition temperature (T_g) of the ionomer is somewhere between 140-170°C and tests at Powercell determined it is thermally stable up to 230°C, meaning that the transfers at 180°C were just above the T_g and at a distance below the degradation temperature. This means that it is unlikely that the ionomer in the CL has been affected. This is reinforced by the fact that a CCM with a HC membrane also experienced the color defect at the elevated temperature. The PFSA membrane previously used has similar thermal properties to the ionomer and the occurrence of the defect without this membrane then suggests that the ionomer is not the affected component.

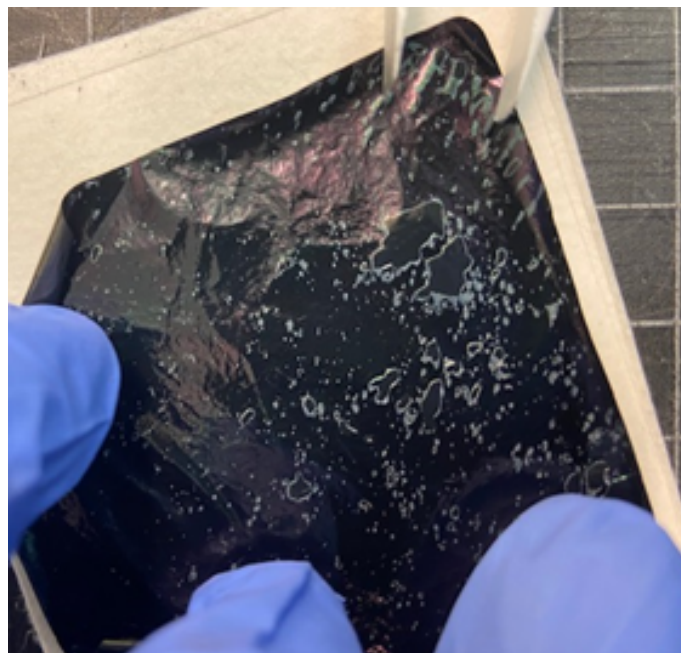


Figure 4.23: Color defect shown on CL surface after CCM assembly at 180°C.

The other theory was that the decal might be the affected component, but since the decal is a commercial product and not all data is available it proved difficult to determine its thermal properties. Although what could be found was that the decal consists of two different layers, one thicker PET film covered by a thinner resin. This also corresponds with the observations made of the affected decals, for example the area inside the red ring in Figure 4.24 shows how the outer layer of the decal has detached and has actually adhered to the CL surface. From this area it can be seen

how it is the outer layer that has not only been detached but is also the one that is affected by the change in color. This then suggests that it is the resin that has been affected by the elevated temperature.

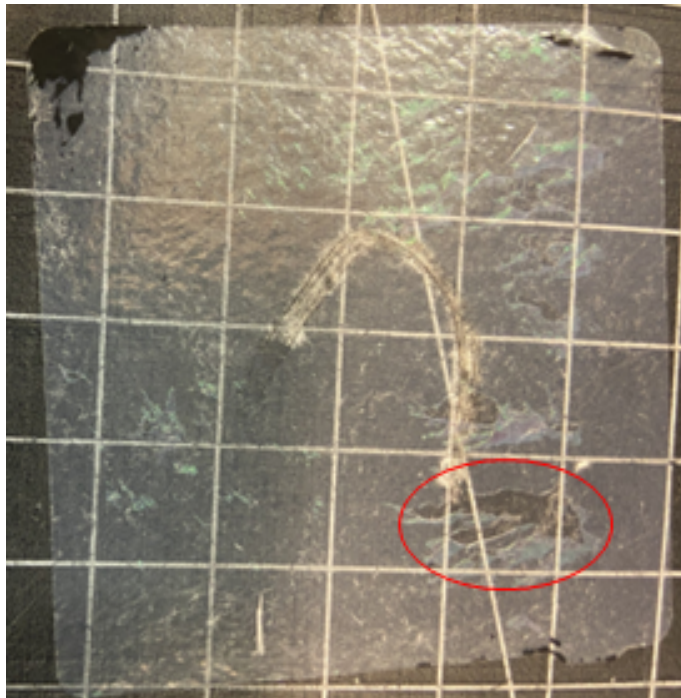


Figure 4.24: Color defect shown on decal after CCM assembly at 180°C.

An additional test was run, to try and confirm that the decal is the affected component. To do so, two CCMs were made using commercial electrodes, which used a different ionomer and decal. Using these electrodes two CCMs with complete transfer and no color defects was achieved at 180°C. As the ionomer of the commercial electrodes has similar thermal properties to the ionomer of in-house electrodes, while the decal is believed to have much more varied properties this result indicates that it is the decal that is affected, when using the in-house electrodes. At a later date it was deduced from the suppliers that the Tg of the resin layer is 160°C and that peeling may occur when used above the Tg, which would concur with the findings in this thesis.

Knowing the Tg of the decal also helped develop a theory for why the occurrence of the color defect on the anode always led to incomplete transfer, but not the other way around. This is believed to be caused by the softening of the decal above its Tg. Because as can be seen in Figure 4.24, the appearance of the color defect is randomized and does not follow any patterns, so as the decal softens at different areas the pressure distribution to the CL is disrupted and this in turn could lead to worse transfer. It is then believed that incomplete transfer occurs when the defect appears on the anode as a result of the anode being thinner than the cathode and the disrupted pressure distribution therefore has a greater effect on the rest of the CCM.

4.6 Evaluation of Pressure Material

After optimising the transfer parameters, they were then used to evaluate the effect of the pressure pad used during the hot-press. A total of three different pressure pads and also the absence of a pressure pad were investigated. The pad material was cellulose, cellulose/polyester mix and polyester for pad 1, 2 and 3 respectively.

4.6.1 Initial tests

As mentioned in previous section, three pressure pads of different materials were investigated in this work. Pad 1 had already been used at Powercell and was known to work in the hot-press, however pad 2 and 3 were new and it was therefore deemed prudent to conduct initial tests to see if they can actually be used in the hot-press. To do this 4 CCMs were prepared, the first three with the different pads and last one without a pressure pad. For these CCMs the same membrane as for the optimization was used, however a PTFE decal and commercial electrodes were used. The reason for the different decal and not using in-house electrodes was that these electrodes were deemed expendable and that the point of this test was not to evaluate the quality of transfer but if the new pads could be used at all. Resulting high intensity light images of each of the four CCMs can be seen in Appendix 1

The cellulose pad has previously been used at Powercell and is known to work in the hot-press, so in these initial tests it was used as a benchmark and to validate that the electrodes were good enough for the CCM assembly. On the anode side the transfer was incomplete, however on the cathode it was a complete transfer. Residuals from the pressure pad could also be seen on the edges of the CCM. The CCM was then investigated using the high intensity light, where the incomplete transfer was very evident in the CCM being quite transparent over many areas. In the same image the imprints left by the decal can also clearly be seen as a square pattern on the CCM. This imprint was one of the reasons why the PTFE decal was not used for the rest of the work.

The second pressure pad tested was of a material consisting of 50/50 cellulose/polyester and as mentioned earlier this material had not been tested at Powercell before. It was therefore of great interest to see if it would work well with distributing the pressure from the press and result in a successful transfer of the electrodes. This first try provided mixed results in this regard, as the anode was a successful transfer whereas the cathode had some transfer, as seen in Figure 4.25. Additionally, in contrast to the cellulose material this pad did not leave any residues on the CCM, which is a desired quality in the pressure pad.

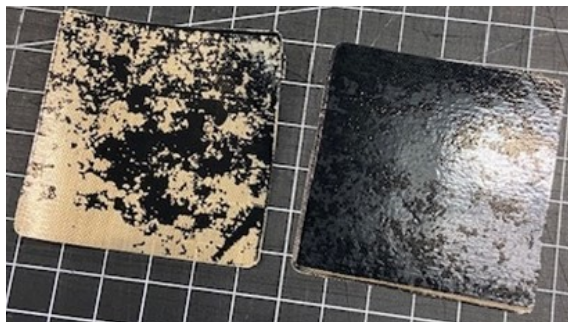


Figure 4.25: Image of decal transfer for CCM assembled using cellulose/polyester pad.

Just as with the previous CCM, this one was evaluated using the high intensity light. The resulting image showed that the transparency of the CCM was comparable to the one assembled using the cellulose pad. The comparable transparency and somewhat successful transfer both indicated that this material could be used as a pressure pad and would therefore be studied further. Although one thing that was noted during the first try and that would have to be remedied during further study can be seen in Figure 4.26. Here it can be seen how the upper part of the pad folded upon itself in-between the heating and cooling of the CCM. This was believed to be part of the reason for the poor transfer of the cathode side, since this was the electrode in contact with the folded pad during the hot-press.

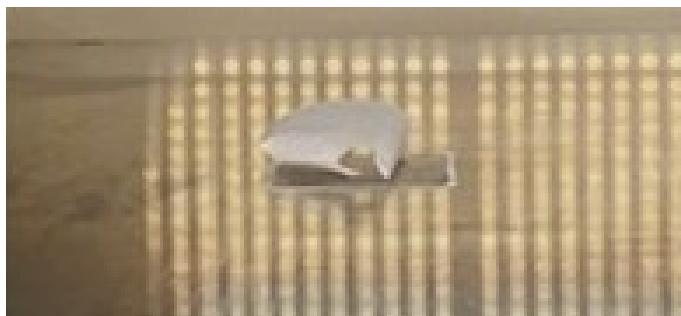


Figure 4.26: Upper pressure pad folded during the hot-pressing.

The third pressure pad tested was made of polyester and just as for the cellulose/polyester material, this had not been used before at Powercell. Using the polyester pad the transfer of the electrodes went similarly to the cellulose/polyester pad, where anode side was transferred completely and the cathode side only had some transfer. However, as can be seen in Figure 4.27, it seems that the CCM assembled with the polyester pad had a bit better transfer than both previously used materials. Moreover, the polyester material, just as the cellulose/polyester material, left no residuals on the CCM.



Figure 4.27: Image of decal transfer for CCM assembled using polyester pad.

From the high intensity light it could also be seen that the CCM is less transparent which indicated that the transfer was better and that this material was of interest for further study as a pressure pad. What should be noted about the polyester pad is that extra care was needed when handling it with the CCM. This as the polyester was more slippery than the other materials and the CCM might move between the pads when preparing for the hot-press.

Lastly a CCM was prepared without the use of a pressure pad. This was done with the intention of confirming the importance of pressure pads for the successful transfer of the electrodes. The resulting transfer was incomplete on the anode side and only had some transfer on the cathode side, meaning this had the worst overall transfer. This was also shown in the high intensity light as this CCM is the most transparent of the four CCMs assembled. This result therefore shows how important the use of a pressure pad is for a successful transfer.

4.6.2 Tests using optimised parameters

With the optimal transfer parameters found for each loading of in-house electrodes, they could then be used to determine how well the alternative materials distribute the pressure and the subsequent transfer. CCMs with a cathode loading of 0.35 mgPt/cm^2 were therefore assembled at $160 \text{ }^\circ\text{C}$ and 600 N/cm^2 , using the two alternative pads. It was noted for both materials that they were too lightweight to keep the CCM in place for the hot-press. This is caused by the higher loading cathode's tendency to bend onto itself and the materials were not heavy enough to keep it down, leading to great misalignment of the different layers in the hot-press. This resulted in non-complete transfers for both materials. It was also noted that pad 3 (polyester) left a clear imprint on the CCM surface, which is undesired. Considering these results and the occurrence of pad 2 folding between heating and cooling during its initial test meant that other alternative pads and weights for pad 2 and 3 had to be explored. The new materials and combinations evaluated is detailed below for each pad material.

4.6.2.1 Cellulose/polyester

As described in previous section, the cellulose/polyester was not heavy enough to weigh down the CCM on its own and a different approach was therefore deemed

necessary. It was decided to try and sandwich this material between the cellulose pad and CCM, as the cellulose has been proved to transfer the electrodes completely and any lack of success would therefore be due to the presence of the cellulose/polyester pad. CCMs at both low and high loading (0.25 and 0.35 mgPt/cm²) were used to test this set-up, which can be seen in Figure 4.28. All CCMs assembled using this set-up gave complete transfer, with no residues or imprints on the CCM, which means that this material is advised to used as an additional layer to the cellulose pad.

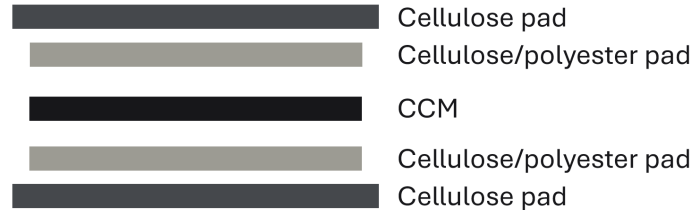


Figure 4.28: Set-up for CCM assembly using cellulose/polyester as sandwich material under the cellulose pad.

4.6.2.2 Polyester

As mentioned in the beginning of this chapter, the polyester pad is not heavy enough to keep the CCM in place during pressing and a weight is therefore needed. For the polyester a metal plate was used as the extra weight, see Figure 4.29. The resulting transfer with this set-up was almost complete. However, the CL that was left on the decal appeared in each corner, suggesting that the distribution of pressure towards the corners was inadequate. The polyester also left imprints on the CCM, as it did when used by itself. Combined with the non-complete transfer the polyester pad was therefore deemed an unsuitable pressure pad material.



Figure 4.29: Set-up for CCM assembly using polyester pad and metal plate.

4.6.2.3 Silicone

A material of interest, due to its possibility for re-use, that it would not leave any residue, and because of its weight, was silicone. Here two types of silicone with varying thickness were used, according to the set-ups shown in Figure 4.30, and they both led to almost complete transfer. However, they also created bubbles underneath the decal during the hot-press where the color defect, discussed in section

4.5, appeared. These two results were then reason enough to discard silicone as a material suitable for pressure pads.

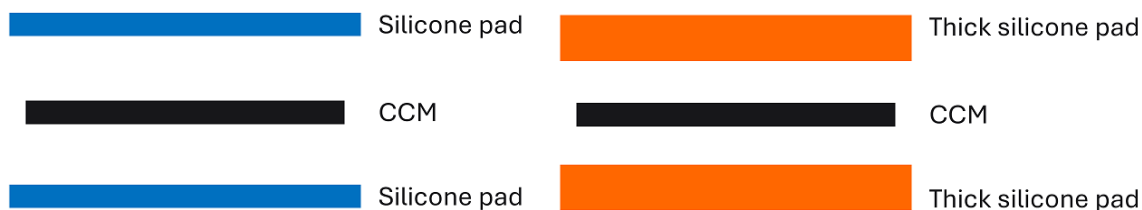


Figure 4.30: Set-up for CCM assembly using two types of silicone pads.

4.6.2.4 Non-reinforced PTFE

Another material chosen for its possibility to re-use and lack of residues was non-reinforced PTFE. Although it is a lighter material compared to silicone and was therefore used as an added layer between the cellulose pad and CCM, see Figure 4.31 for the set-up. Initial tests gave complete transfers and re-usage of the material showed comparable transfer. However, this was done with the lower loading of 0.25 mgPt/cm^2 and further tests were therefore conducted with the high loading of 0.35 mgPt/cm^2 . These gave only almost complete transfer, meaning it is not optimal to use this material since it does not work for each loading.

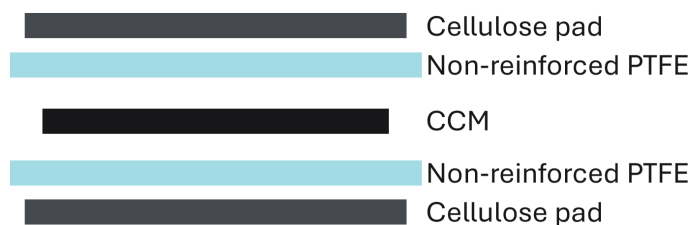


Figure 4.31: Set-up for CCM assembly using non-reinforced PTFE as sandwich material under the cellulose pad.

4.6.2.5 Non-residual paper

The last material investigated was a non-residual paper material, which was used similarly to the non-reinforced PTFE, see Figure 4.32. The idea was that this material was to prevent cellulose residues on the CCM by acting as a physical barrier, while not disturbing the pressure distribution. The CCMs assembled with this set-up all gave complete transfer, even at high loading, and no residue could be seen on the CCM. This means that this material is appropriate to use as an additional layer to the already used and studied cellulose pressure pad. It is also advised to be used over the cellulose/polyester pad, which also gave complete transfer, due to its better availability and ease of handling.

4. Results



Figure 4.32: Set-up for CCM assembly using non-residual paper as sandwich material under the cellulose pad.

4.7 In-situ Measurements

Four in-situ tests were made, where three tests used a CCM from each loading that had achieved complete transfer at the optimal parameters found and one test used a previously verified MEA as reference sample. The resulting polarisation and resistance curves can be seen in Figure 4.33, where the green line is the reference MEA and blue, red, and yellow corresponds to the low, middle, and high loading.

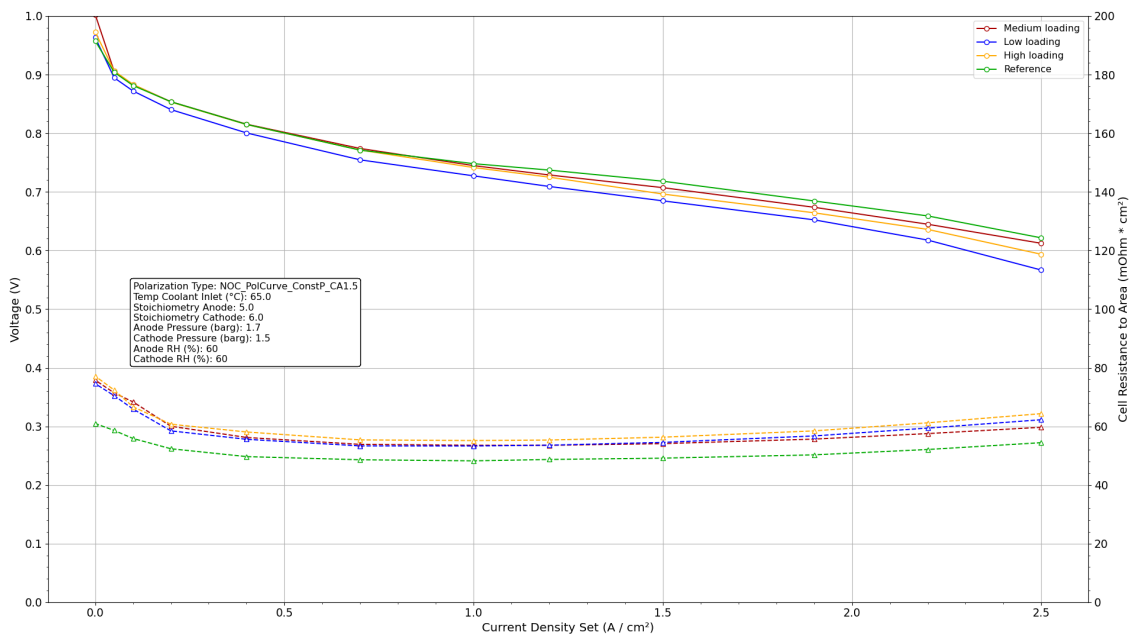


Figure 4.33: Illustration of resulting polarization and resistance curves from in-situ testing.

At the OCV all four MEAs are above 0.9 V, which would indicate that there were no great leakages or pinholes present in the samples. In the kinetic region the lower loading proved to have a lower performance, which was expected since this region is dominated by the reaction kinetics and less platinum at the cathode would therefore mean a lower performance. Interestingly this did not occur when comparing the middle to high loading, as these can be seen to have had a similar performance in

the kinetic region. This was likely due to poor utilization of the catalyst in the higher loading, which would be a consequence of the electrode quality and not dependent on the assembly parameters. Then in the ohmic region, the middle loading can be seen to have performed better than the high loading and yet again this was likely due to the quality of the electrodes used. Looking at the resistance curves at the bottom of Figure 4.33 the reference MEA can be seen to have exhibited a lower resistance than the three sampled CCMs. From the three CCMs the high loading proved to have the highest resistance, which would correspond to its greater loss in the ohmic region of the polarization curve. What can be deduced from these results is that, while the electrode quality still needs to be improved, the optimal transfer parameters found and used to assemble the three sampled CCMs also result in a comparatively good and well-functioning MEA. The results also showed that it could be of interest to perform a statistical analysis on the CCMs assembled at these parameters, to better evaluate the effect of the loading on the performance.

5

Conclusion

Based on the results in this thesis, several conclusions related to the initial objectives can be drawn. Regarding the optimization of transfer parameters the results can be seen in Table 5.1, where the optimal parameters were found for the PFSA membrane with all three loadings and the smaller area. For the HC membrane and the increased area of 280 cm² only indications of the optimal parameters, given in the table, could be established.

Table 5.1: Optimal transfer parameters.

Membrane	Loading (mgPt/cm ²)	Area (cm ²)	Pressure (N/cm ²)	Temperature (°C)
PFSA	0.25	25	450	160
PFSA	0.3	25	600	160
PFSA	0.35	25	600	160
PFSA	0.25	280	450	160
PFSA	0.3	280	600	160
PFSA	0.35	280	600	160
HC	0.3	25	900	160
HC	0.35	25	900	160

Using the optimal parameters found the influence of different pressure pad materials could be investigated, where the non-residual paper material proved to work best as an additional material to the already used cellulose pads. While optimising the parameters and evaluating the pressure pads different analytical tools were also investigated. From this investigation it can be concluded that the high intensity light is the advised analytical tool to be used during CCM assembly. This is due to its quick and easy use, and sensitivity to defects.

6

Outlook for Further Work

This thesis has served to expand the knowledge regarding CCM quality assessment and assembly in a number of different ways, yet there are still many areas that needs further research to fully understand their impact on quality and to further optimize the CCM assembly.

Due to shortage of material, the full matrices planned for the bigger CCMs with PFSA membrane could not be completed. Complete transfer was achieved for two CCMs, for each loading, however additional CCMs would need to be assembled at the same parameters to fully confirm the optimal parameters indicated by these results. The same goes for the CCMs assembled with a HC membrane, where only the parameters for CCMs with a 0.3 mgPt/cm^2 loading and 25 cm^2 area can be deemed confirmed. To confirm the optimal parameters of the other loadings and the bigger area additional CCMs, based on the results of this thesis, needs to be assembled.

Based on the results regarding the investigation of analytical tools for the CCM quality check, the high intensity light method was concluded to be the advised tool. However, the results also show that further research is needed to fully understand what defects are shown with this method. A suggestion for this would be to use pristine and non-defected electrodes and introduce artificial defects such as holes to them. By doing this to both an anode and cathode, the defects shown in the intense light can be further understood by aligning the defected electrodes to different degrees. It can then be deducted how miss-aligned or how far away two defects can occur and still be visible in the intense light images. This comes as this thesis has shown that pinholes and fully aligned missing CL defects are clearly shown in the high intensity light images, but it has also been suggested that partly and nearly aligned missing CL can also be shown. The investigation of artificially introduced defects could then serve to confirm this hypothesis.

The use of the high intensity light showed that there was a significant amount of defects on the majority of electrodes used in this thesis, with the worst quality apparent on the cathodes. This lack of quality also became apparent during the in-situ testing, which means that the defects shown actually seems to have had an impact on the performance of the assembled MEAs. Since this can not be avoided or mitigated during the assembly process, further research into the increased quality of the in-house electrodes is therefore advised.

For the in-situ testing it could also be of interest to conduct a statistical anal-

ysis into effect of the cathode loading on the performance of the MEAs. For this thesis there was only time to analyze one CCM for each loading, which is not enough to draw any reliable conclusions on the individual loadings effect. However, since the optimal transfer parameters were found in this thesis they can now be used to expand upon the in-situ testing and properly evaluate the loadings effect.

From the investigation into the effect of different pressure pad materials, it was advised that the non-residual paper material was to be used for further CCM assembly. Using this material would however not exclude the usage of the previously used cellulose pad, as it would be used as an additional layer. This means that, even if it not by much, more time and material would be required for the CCM assembly. If this is undesired by the assembler it can then be proposed to continue the investigation into other materials that can work instead of the cellulose pad, and not additionally to it. Further research could also be done into the potential re-usage of both cellulose pads and non-residual paper, as reusing the materials would save both time and money.

To further optimize the amount of time and energy spent for each assembled CCM, an investigation into the maximum transferable area using in-house electrodes would be of interest. In this thesis the largest CCM assembled with in-house electrodes had an area of 280 cm^2 and no attempts at larger CCMs with these electrodes were attempted. However, a CCM with an area of 735 cm^2 was assembled using commercial electrodes and this result indicates that with further optimization the in-house electrodes should also be able to be used at this size.

Bibliography

- [1] Bee Huah Lim et al. “Comparison of catalyst-coated membranes and catalyst-coated substrate for PEMFC membrane electrode assembly: A review”. In: *Chinese Journal of Chemical Engineering* 33 (2021), pp. 1–16. ISSN: 1004-9541. DOI: <https://doi.org/10.1016/j.cjche.2020.07.044>. URL: <https://www.sciencedirect.com/science/article/pii/S1004954120304158>.
- [2] Frano Barbir. “Chapter Four - Main Cell Components, Material Properties, and Processes”. In: *PEM Fuel Cells (Second Edition)*. Ed. by Frano Barbir. Second Edition. Boston: Academic Press, 2013, pp. 73–117. ISBN: 978-0-12-387710-9. DOI: <https://doi.org/10.1016/B978-0-12-387710-9.00004-7>. URL: <https://www.sciencedirect.com/science/article/pii/B9780123877109000047>.
- [3] Xiaolu Liang et al. “A modified decal method for preparing the membrane electrode assembly of proton exchange membrane fuel cells”. In: *Fuel* 139 (2015), pp. 393–400. ISSN: 0016-2361. DOI: <https://doi.org/10.1016/j.fuel.2014.09.022>. URL: <https://www.sciencedirect.com/science/article/pii/S0016236114008825>.
- [4] S. A. Ogu-Egede. *Fuel Cell Membrane Electrode Assembly - Fabrication and Characterization*. Politecnico di Torino. 2022. URL: <http://webthesis.biblio.polito.it/id/eprint/24233>.
- [5] D. Schulz. “Exploring the process design and parameters for a fuel cell membrane electrode assembly by decal transfer”. MA thesis. Chalmers University of Technology, 2023. URL: <http://hdl.handle.net/20.500.12380/306931>.
- [6] Frano Barbir. “Chapter One - Introduction”. In: *PEM Fuel Cells (Second Edition)*. Ed. by Frano Barbir. Second Edition. Boston: Academic Press, 2013, pp. 1–16. ISBN: 978-0-12-387710-9. DOI: <https://doi.org/10.1016/B978-0-12-387710-9.00001-1>. URL: <https://www.sciencedirect.com/science/article/pii/B9780123877109000011>.
- [7] S. H. Akella et al. “Studies on structure property relations of efficient decal substrates for industrial grade membrane electrode assembly development in PEMFC”. In: *Sci Rep* 8 (2018), p. 12082. DOI: [10.1038/s41598-018-30215-0](https://doi.org/10.1038/s41598-018-30215-0). URL: <https://doi.org/10.1038/s41598-018-30215-0>.
- [8] Xiao-Zi Yuan et al. “A review of functions, attributes, properties and measurements for the quality control of proton exchange membrane fuel cell components”. In: *Journal of Power Sources* 491 (2021), p. 229540. ISSN: 0378-7753. DOI: <https://doi.org/10.1016/j.jpowsour.2021.229540>. URL: <https://www.sciencedirect.com/science/article/pii/S0378775321000872>.

- [9] Marc-Antoni Goulet et al. “Mechanical properties of catalyst coated membranes for fuel cells”. In: *Journal of Power Sources* 234 (2013), pp. 38–47. ISSN: 0378-7753. DOI: <https://doi.org/10.1016/j.jpowsour.2013.01.128>. URL: <https://www.sciencedirect.com/science/article/pii/S0378775313001857>.
- [10] Shuai Mo, Lin Du, Zhen Huang, et al. “Recent Advances on PEM Fuel Cells: From Key Materials to Membrane Electrode Assembly”. In: *Electrochem. Energy Rev.* 6 (2023), p. 28. DOI: 10.1007/s41918-023-00190-w. URL: <https://doi.org/10.1007/s41918-023-00190-w>.
- [11] Yilser Devrim and Ayhan Albostan. “Enhancement of PEM fuel cell performance at higher temperatures and lower humidities by high performance membrane electrode assembly based on Nafion/zeolite membrane”. In: *International Journal of Hydrogen Energy* 40.44 (2015). The 4th International Conference on Nuclear and Renewable Energy Resources (NURER2014), 26-29 October 2014, Antalya, Turkey, pp. 15328–15335. ISSN: 0360-3199. DOI: <https://doi.org/10.1016/j.ijhydene.2015.02.078>. URL: <https://www.sciencedirect.com/science/article/pii/S0360319915004589>.
- [12] Suzanne E Fenton et al. “Per-and Polyfluoroalkyl Substance Toxicity and Human Health Review: Current State of Knowledge and Strategies for Informing Future Research”. In: *Environmental Toxicology and Chemistry* 40.3 (Mar. 2021). Epub 2020 Dec 7, pp. 606–630. DOI: 10.1002/etc.4890.
- [13] *EUR-Lex - Access to European Union Law*. EUR-Lex. URL: <https://eur-lex.europa.eu/legal-content/EN/TXT/?uri=COM:2020:667:FIN> (visited on 04/23/2024).
- [14] M.P. Arcot et al. “Investigation of catalyst layer defects in catalyst-coated membrane for PEMFC application: Non-destructive method”. In: *International Journal of Energy Research* 42.11 (2018), pp. 3615–3632. DOI: <https://doi.org/10.1002/er.4107>. eprint: <https://onlinelibrary.wiley.com/doi/pdf/10.1002/er.4107>. URL: <https://onlinelibrary.wiley.com/doi/abs/10.1002/er.4107>.
- [15] Muneendra Prasad Arcot et al. “Morphological Characteristics of Catalyst Layer Defects in Catalyst-Coated Membranes in PEM Fuel Cells”. In: *Electrochem* 4.1 (2023), pp. 1–20. ISSN: 2673-3293. DOI: 10.3390/electrochem4010001. URL: <https://www.mdpi.com/2673-3293/4/1/1>.
- [16] Sang Moon Kim et al. “High-performance Fuel Cell with Stretched Catalyst-Coated Membrane: One-step Formation of Cracked Electrode”. In: *Scientific reports* 6 (May 2016), p. 26503. ISSN: 2045-2322. DOI: 10.1038/srep26503. URL: <https://europemc.org/articles/PMC4876450>.
- [17] S. Kundu et al. “Morphological features (defects) in fuel cell membrane electrode assemblies”. In: *Journal of Power Sources* 157.2 (2006). Selected papers presented at the Ninth Grove Fuel Cell Symposium, pp. 650–656. ISSN: 0378-7753. DOI: <https://doi.org/10.1016/j.jpowsour.2005.12.027>. URL: <https://www.sciencedirect.com/science/article/pii/S0378775305016964>.
- [18] Jonas Stoll et al. “Impacts of cathode catalyst layer defects on performance and durability in PEM fuel cells”. In: *Journal of Power Sources* 583 (2023),

- p. 233565. ISSN: 0378-7753. DOI: <https://doi.org/10.1016/j.jpowsour.2023.233565>. URL: <https://www.sciencedirect.com/science/article/pii/S0378775323009412>.
- [19] Suhui Ma et al. “Delamination evolution of PEM fuel cell membrane/CL interface under asymmetric RH cycling and CL crack location”. In: *Applied Energy* 310 (2022), p. 118551. ISSN: 0306-2619. DOI: <https://doi.org/10.1016/j.apenergy.2022.118551>. URL: <https://www.sciencedirect.com/science/article/pii/S030626192200037X>.
- [20] Yanzhou Qin et al. “Modeling the membrane/CL delamination with the existence of CL crack under RH cycling conditions of PEM fuel cell”. In: *International Journal of Hydrogen Energy* 46.12 (2021), pp. 8722–8735. ISSN: 0360-3199. DOI: <https://doi.org/10.1016/j.ijhydene.2020.12.043>. URL: <https://www.sciencedirect.com/science/article/pii/S0360319920345778>.
- [21] Michael Ulsh et al. ““The development of a through-plane reactive excitation technique for detection of pinholes in membrane-containing MEA sub-assemblies””. In: *International Journal of Hydrogen Energy* 44.16 (2019), pp. 8533–8547. ISSN: 0360-3199. DOI: <https://doi.org/10.1016/j.ijhydene.2018.12.181>. URL: <https://www.sciencedirect.com/science/article/pii/S0360319918341855>.
- [22] Adam Z. Weber. “Gas-Crossover and Membrane-Pinhole Effects in Polymer-Electrolyte Fuel Cells”. In: *Journal of The Electrochemical Society* 155.6 (Apr. 2008), B521. DOI: [10.1149/1.2898130](https://doi.org/10.1149/1.2898130). URL: <https://dx.doi.org/10.1149/1.2898130>.
- [23] MohammadAmin Bahrami et al. “Improved Decal Transfer Method to Reduce Membrane Damage from Foreign Particles in Membrane Electrode Assembly”. In: *Journal of The Electrochemical Society* 170.11 (Nov. 2023), p. 114527. DOI: [10.1149/1945-7111/ad0dc3](https://doi.org/10.1149/1945-7111/ad0dc3). URL: <https://dx.doi.org/10.1149/1945-7111/ad0dc3>.
- [24] A. Di Gianfrancesco. “8 - Technologies for chemical analyses, microstructural and inspection investigations”. In: *Materials for Ultra-Supercritical and Advanced Ultra-Supercritical Power Plants*. Ed. by Augusto Di Gianfrancesco. Woodhead Publishing, 2017, pp. 197–245. ISBN: 978-0-08-100552-1. DOI: <https://doi.org/10.1016/B978-0-08-100552-1.00008-7>. URL: <https://www.sciencedirect.com/science/article/pii/B9780081005521000087>.
- [25] Jian Zhao, Huiyuan Liu, and Xianguo Li. “Structure, Property, and Performance of Catalyst Layers in Proton Exchange Membrane Fuel Cells”. In: *Electrochemical Energy Reviews* 6.1 (2023), p. 13. ISSN: 2520-8136. DOI: [10.1007/s41918-022-00175-1](https://doi.org/10.1007/s41918-022-00175-1). URL: <https://doi.org/10.1007/s41918-022-00175-1>.

A

Appendix 1

High intensity light image of CCMs prepared using a cellulose pad, cellulose/polyester pad, polyester pad and no pad.



DEPARTMENT OF PHYSICS
CHALMERS UNIVERSITY OF TECHNOLOGY
Gothenburg, Sweden
www.chalmers.se



CHALMERS
UNIVERSITY OF TECHNOLOGY